MODELING SOIL MOISTURE FROM REAL-TIME WEATHER DATA

BY

EMMANNUEL ROTIMI OJO

A Thesis submitted to the Faculty of Graduate Studies of the University of Manitoba in partial fulfillment of the requirements for the degree of

MASTER OF SCIENCE

Department of Soil Science

University of Manitoba

Winnipeg, Manitoba

ABSTRACT

Ojo, Emmanuel Rotimi. M.Sc., The University of Manitoba, February, 2012. Modeling Soil Moisture from Real-Time Weather Data. Major Professor; Paul R. Bullock.

Extreme variability of rainfall during the growing season in the Prairies underlies the need to improve means of quantifying the amount of soil moisture available for plant growth in real time. This study was conducted to modify and validate the Versatile Soil Moisture Budget (VSMB) for estimating volumetric soil water content. A network of soil moisture hydra probes and weather stations were installed for continuous soil moisture monitoring and real-time weather data collection at 13 sites across Central and Western Manitoba during the 2009 and 2010 growing seasons. The data from the probes were validated and calibrated. Both the laboratory and field validations showed that the root mean square error of the default factory calibration increased with increasing clay content of the soil. Outputs from these probes were used to test the modified VSMB model. The model was most effective at simulating soil water content at the surface layers.

ACKNOWLEDGEMENTS

I would like to express my appreciation to all the members of my M.Sc. committee; Dr Paul Bullock, Dr Oluwole Akinremi and Dr Rob Gulden for their constant support and advice. I am always awestruck at their inestimable depth of knowledge and experience. Also, I am extremely grateful to Dr Paul Bullock for the opportunity to conduct my research under his direct supervision. I cherish his cognitive leadership and inter-personal skills which I enjoyed and learnt. They are rare golden treasures.

Thank you to the entire technical, academic and support staff in the Department for all their assistance, and also, to my innumerable cloud of friends at the Soil Science Department (*soilies*) especially Jean- my summer student, Ike and Taryn; Graduate Student Association, International Center for Students and Church of the Rock - being a part of you has been a wonderful experience for me.

I am grateful to the Manitoba Government for the Manitoba Graduate Scholarship that I received as well as the Drought Research Initiative (DRI) and Agriculture and Rural Development Initiative (ARDI) for their monetary support for this project.

Special thanks to my lovely parents, siblings, in-laws and my fiancée for your constant support and for believing in me. You are the best! And to Sewa, my first niece, thanks for giving me great inspiration and joy.

“People that made ground-breaking discoveries do not have two heads. You can do whatever anyone is doing and be better at it with God’s help” - Rev A. O. Ojo

This Masters of Science Thesis is dedicated to Rev. Amos O. Ojo and Mrs Florence A. Ojo, my wonderful parents. Drinking from your cistern of wisdom and growing under your tutelage is what moulds me to the person I am. I would be forever thankful for your awesome parenting and guidance. God bless you.

TABLE OF CONTENTS

Page

5. OVERALL SYNTHESIS

6. APPENDICES

LIST OF TABLES

LIST OF FIGURES

Figure Page

LIST OF ABBREVIATIONS

AET	Actual Evapotranspiration
ET	Evapotranspiration
ET_o	Reference Evapotranspiration
FAO-56	Penman-Monteith ET_o Procedure
MBE	Mean Bias Error
PT	Priestley-Taylor
RMSE	Root Mean Square Error
VB_0	Current VSMB
VB_1	Modified VSMB
VSMB	Versatile Soil Moisture Budget
ε	Real Dielectric Permittivity
ε_{TC}	Temperature Corrected Real Dielectric Permittivity

1 INTRODUCTION

Weather, Water and Agriculture

Water plays a very significant role in nearly all earth processes and one of the most anthropogenically-significant aspects of the water cycle is soil moisture. The extreme variability of weather parameters especially rainfall is a major meteorological driver that influences soil water dynamics. The occurrence of drought and flood are reflected in soil moisture variation. The location and timing of extreme weather events such as hailstorms and tornadoes have even been linked to variability in soil moisture (Hanesiak et al. 2004).

A major component of weather is precipitation. The earth surface receives precipitation mainly in the form of rainfall or snowfall which then melts on the earth's surface. The water received on the earth's surface must follow one of two pathways. A portion of it is soaked up by the soil as infiltration with some of this infiltrated portion added to the groundwater system while that held in the rhizosphere (region of the soil that is directly influenced by plant root) can be used by plants to meet their physiological needs. The surface water that does not infiltrate runs off the surface and into surface water bodies. The water in rivers and other large water bodies as well as the pores of surface soil is transformed from liquid to water vapor in a process called evaporation while the water vapor transferred to the atmosphere via plant stomata is called transpiration. Rising air currents transport the water vapour up into the

atmosphere where it cools, condenses and falls back to the earth's surface as precipitation for a repeated cycle.

Agrometeorology is the study of the influence of weather on agriculture with the main objective of using this knowledge to increase agricultural productivity. Monteith (2000) noted that attempts to relate agricultural production to weather can be dated back to at least 2000 years ago. Since crops were first cultivated, farmers have acknowledged the overriding importance of weather in setting both potential and achieved levels of production. Monteith (2000) further noted that mainly qualitative studies in the 19th century were followed by statistical analyses, then by microclimatic measurement and most recently by modeling. A survey was conducted on the distribution of papers in the Agricultural and Forest Meteorology journal between December 1964 to June 1972; and from June 1996 to June 1998. Each period covered about 190 papers that were divided into 18 sub-categories. Of these sub-categories, both periods had the highest proportion of papers on water balance; 22.5% and 24.8% respectively. However, in the span of 34 years, papers on modeling increased from 1.2% in the first period to 19.4% in the second period (Monteith, 2000). This depicts the increasing interest in and number of agrometeorological models in the area of agrometeorology in the last half of the 20^{th} century.

To account for the impact of weather variability on crop production, agrometeorological variables are key inputs required for the operation of crop simulation models (Hoogenboom, 2000). Excess or deficit of plant available water is one of the most important factors that determine crop growth and

development which ultimately limits crop yield. The extreme variability of weather poses a challenge to agricultural production and to the science of agrometeorology. The Canadian prairies (southern region of Alberta, Saskatchewan and Manitoba) are prone to extreme meteorological events such as droughts and floods. Within the span of a decade, the Prairies have experienced one of the worst droughts on record from 1999 through 2005 (Gervais, 2008) as well as extreme flooding in 2009 and 2010. In 2010, an estimated 8 million acres of land was not seeded in Saskatchewan (30% of the provincial farmland) and another 4 million acres of crop was lost to flooding after receiving 150 per cent of normal precipitation with many areas in the province getting well over 200 per cent of normal precipitation (Saskatchewan Government, 2010). From 1971 to 2004, the Canadian Prairies had the lowest water yield and the highest variability in water yield when compared to other parts of the country. This variability is of interest because lack of predictability in the flows of renewable water resources affects economic activities, including water for irrigation of agricultural land (Statistics Canada, 2010).

Soil Moisture Monitoring and Versatile Soil Moisture Budget

Despite the critical role of soil moisture for agriculture, flood risk and severe weather, efforts to establish a continuous soil moisture monitoring network have been limited. Soil water sensors that provide continuous real time data are expensive and often require soil-specific calibration which is labour

intensive. Calibration or the verification of sensor output using known standardized methods is vital in ensuring that the sensor measurements accurately depict real world observations. The dynamic and variable nature of soil moisture content requires a dense network of sensors in order to provide a reasonable level of accuracy in the estimation of soil moisture conditions across any given area. Thus, most of the soil moisture sensor networks in the Prairies are for research purposes.

Since 2005, there has been a dramatic increase in the number of automated weather stations on the Prairies that report weather data in real time. There is a great potential to use models to estimate soil moisture content from the information provided by these weather stations as well as the soil information of the area. One such model is the Versatile Soil Moisture Budget or VSMB (Baier and Robertson, 1966). VSMB was selected for this study because of its robust, physically-based nature and its ability to simulate soil moisture content throughout the root-zone with several user-defined soil horizons and differing soil water characteristics, which is a condition that is typical in many Prairie soils. Since the time of its development, various components of the VSMB have been modified and validated under several conditions (Baier et al 1979; De Jong 1988; Boisvert et al 1992; Hayhoe et al 1993) and adapted for various uses like irrigation scheduling (Boisvert et al 1990), estimation of field workdays in Canada (Baier, 1973) and spring wheat yield prediction (Akinremi and McGinn 1996). Akinremi and McGinn (1996) used the VSMB to improve the accuracy of water

balance estimates of the Palmer Drought Index (PDI); a model used to predict wheat yield reductions associated with drought in the Canadian prairies.

Objectives

Although the cost of establishing a network of *in* situ soil moisture sensors is prohibitive, it is still necessary to measure soil moisture content at some locations to ensure that accurate data is available to validate estimates generated from models. Thus, the first objective of this study was to determine the accuracy of the output from a specific type of soil moisture sensor (the Stevens' hydra probe) compared to measured volumetric (gravimetrically derived) soil moisture in different soil textures. The purpose was to ensure that the hydra probes were providing acceptable accuracy so that they could be used to test the soil moisture output from the VSMB.

The second objective was to modify the evapotranspiration component of the current version of VSMB (Akinremi et al. 1996) by replacing the Priestley-Taylor derived ET_o with the Penman-Monteith (PM) ET_o. The PM ET_o has been widely used and found to give a better estimate of reference evapotranspiration than the PT (Suleiman and Hoogenboom 2007, Droogers and Allen 2002). The ability to utilize the VSMB with a PM ET_o was made possible with the increase in the number of weather stations that report additional weather parameters like wind speed, humidity and solar radiation rather than just air temperature as was most common in the past.

The third objective was to validate the modified VSMB model by comparing the modeled soil moisture output to that from the field calibrated soil moisture sensors.

Monitoring soil water and providing real-time estimates is vital to understanding drought, floods as well as weather forecasting on a county, provincial and national basis. Thus, results from this study can be used to improve flood forecasting and to enhance agricultural management decisions affected by soil moisture such as irrigation scheduling and timing of various farming operations like planting, fertilizer application, pest and disease control.

References

Akinremi, O.O. and McGinn, S.M. 1996. Usage of soil moisture models in agronomic research. Can. J. Soil Sci., **76:** 285–29.

Akinremi, O.O., McGinn, S.M. and Barr, A.G. 1996. Simulation of soil moisture and other components of the hydrological cycle using a water budget approach. Can. J. Soil Sci., **75**: 133-142.

Baier, W. and Robertson, G.W. 1966. A new versatile soil moisture budget. Can. J. Plant Sci., **46**: 299–315.

Baier, W. 1973. Estimation of field work days in Canada from the versatile soil moisture budget. Can. Agric. Eng., **15**:84-87.

Baier, W., Dyer, J.A. and Sharp, W.R. 1979. The versatile soil moisture budget. Tech. Bull. 87, Agrometeorology Section, Research Branch, Agriculture Canada, Ottawa, ON. 52 pp.

Boisvert, J.B., Bootsma, A., Dwyer, L.M. and Brewin, D. 1990. IRRIGATE: User guide for irrigation management by computer. Tech. Bull. 1990-2E, Agrometeorology Section, Research Branch, Agriculture Canada, Otttawa, ON. 65 pp.

Boisvert, J.B., Dyer, J.A., Lagace, R. and Dube, P.A. 1992. Estimating water table fluctuations with a daily weather-based budget approach. Can. Agric. Eng., **32**: 115–124.

De Jong, R. 1988. Comparison of two soil-water models under semi-arid growing conditions. Can. J. Soil Sci., **68**: 17–27.

Droogers, P. and Allen, R.G. 2002. Estimating Reference Evapotranspiration under Inaccurate Data Conditions. Irrigation and Drainage Systems, **16**: 33-45.

Gervais, D.M. 2008. Assessment of the Second-Generation Prairie Agrometeorological model's performance for spring wheat on the Canadian Prairies. M.Sc. Thesis, University of Manitoba. [Online] Available: [2010 December 23]

Hanesiak, J.M., Raddatz, R.L. and Lobban, S. 2004. Local initiation of deep convection on the Canadian Prairie provinces. Boun. Layer Met. **110**: 455-470.

Hayhoe, H.N., Pelletier, R.G. and Van Vliet, L.P.J. 1993. Estimation of snowmelt runoff in the Peace River region using a soil moisture budget. Can. J. Soil Sci., **73**: 489–501.

Hoogenboom, G. 2000. Contribution of agrometeorology to the simulation of crop production and its applications. Agricultural and Forest Meteorology, **103**: 137-157.

Monteith, J.L. 2000. Agricultural Meteorology: evolution and application. Agricultural and Forest Meteorology, **103**: 5-9.

Saskatchewan Government, Ministry of Agriculture. 2010. Excess Moisture Program Fact Sheet. [Online] Available: http://www.saskcropinsurance.com/Default.aspx?DN=82213e54-86c9-410a-b285-4d641a5b894c [2010 December 21].

Statistics Canada. 2010. Study: Freshwater supply and demand in Canada 1971 – 2005, Trends in water yield on the Prairies. [Online] Available: http://www.statcan.gc.ca/daily-quotidien/100913/dq100913b-eng.htm [2010 December 22]

Suleiman, A.A. and Hoogenboom, G. 2007. Comparison of Priestley-Taylor and FAO-56 Penman-Monteith for Daily Reference Evapotranspiration Estimation in Georgia. J. Irrig. and Drain. Engrg, **133**: 175-182.

2. Calibration of Frequency Domain Reflectometry Probes

2.1 Abstract

The value of soil moisture content for a broad range of applications has led to the development of many different soil moisture sensors. Frequency domain reflectometers (FDR) are instruments that can be deployed for *in situ* soil moisture measurements and tracked with a data logger. These probes measure the dielectric permittivity of the soil, a parameter that depends mainly on the soil moisture content. This provides high frequency updates on soil moisture status, which are critical for the development and testing of other methods for soil moisture determination, such as models and remote sensing.

A total of 13 soil moisture monitoring site-years were established using FDR sensors (Steven's hydra probes) in central and eastern Manitoba in 2009 and 2010 for the purpose of testing soil moisture models. Prior to their deployment in the field, each hydra probe was tested using a laboratory validation technique to ensure that they performed uniformly under controlled conditions based on the default factory calibration. Four soil types were tested in the laboratory with varying percent clay content and the default factory calibration performed very well in medium textured soils (20-40% clay content) with a Root Mean Square Error (RMSE) of 0.006m^3 m^{-3} and Mean Bias Error (MBE) of 0.002 when compared to the volumetric water content. However, soils with 40-60% and > 60% clay content had higher RMSE of 0.030m^3 m^{-3} and 0.054m^3 m^{-3} respectively. Thereafter, the probes were deployed to the field. At each of the

monitoring sites, four hydra probes were installed to monitor moisture levels at 4 depths (5, 20, 50 and 100 cm) for a total of 52 site-depths. The real dielectric permittivities of the soil were fitted to volumetric soil moisture content to generate field based calibration equations and were compared to the default factory calibration. The site-depths were binned into four types (0-20%, 20-40%, 40-60%, >60% clay) and the coefficient of determination between the observed and the default factory values obtained were 0.83, 0.58, 0.38 and 0.49 respectively. This showed that R^2 decreased with increasing clay content except between the third and fourth categories. The RMSE values, 0.041, 0.069, 0.99 and 0.075 m^3 m^{-3} showed a similar trend. The result reinforces the need for soil-specific calibration of FDR sensors especially in soils with high clay content.

2.2 Introduction

In the global distribution of water, oceans constitute about 97.25%, ice 2%, groundwater 0.7% and all other water 0.05%. However, 33% of the other water is held as soil moisture, 60% in lakes, 6% in the atmosphere and 1% in rivers (Brady and Weil, 1999). Though all these water pathways are vital for global energy balance and human comfort, soil moisture can be argued to have the most direct impact on agriculture. Soil moisture can simply be defined as the water held in the vadose zone- unsaturated zone between the earth's soil surface and the water table. However, the exact definition can vary depending on the context in which it is used (Seneviratne et al 2010).

Several attempts have been made to quantify soil moisture. Landa and Nimmo (2003) reported that between the close of the 19th century and mid-20th century, Lyman Briggs made many significant contributions to the understanding of soil-water and plant-water interactions. He published an explanation of the roles of surface tension and gravity in determining the state of soil moisture (Briggs, 1897). Though many techniques have been developed that relate specific soil properties to the amount of water in the soil, the standard method for quantifying soil moisture is the thermo-gravimetric method which requires oven drying a known volume of soil at 105 ^{o}C and determining the weight loss. This method has significant limitations because it is time consuming, labour intensive and destructive to the sampled soil, meaning that it cannot be used for repeated measurement at the same location. However, it is indispensable as a standard method for calibration and evaluation purposes (Robock et al., 2000, Walker et al. 2004, and Robinson et al., 2008).

In situ monitoring of soil moisture is a challenging task in hydrology (Topp, 2003). Many indirect methods have been developed to quantify soil moisture including measurements based on the dielectric properties of a soil volume, namely, Time Domain Reflectometry (TDR) and Frequency Domain Reflectometry (FDR).

The dielectric methods relate changes in the water content of soil to the dielectric constant of the medium. Water has a high dielectric constant of 80 compared to that of dry soil which ranges from 3-5 and air which has a dielectric constant of 1. TDR utilizes a pair of metal rods connected to a signal receiver

and inserted into the soil. The rods serve as conductors while the soil around the rods serves as the dielectric medium. A voltage signal is sent through the rod into the soil and it is reflected back to the TDR receiver. A device measures the time between sending and receiving the signal which is related to the dielectric constant of the medium which is mainly a function of the amount of water that is present in the soil. The propagation velocity of the signal decreases as the water content increases. Thus, the time interval between sending and receiving a signal increases as the soil water content increases. Hook and Livingston (1996) showed that a dominant source of error in estimating soil water content using TDR was the uncertainty in determining the propagation travel time (Lin, 2003). To overcome this limitation, the FDR was developed. A FDR probe uses an oscillator to generate an AC field which is applied to the soil. The soil forms the dielectric of a capacitor which works with the oscillator to form a tuned circuit. A change in soil water content causes a shift in frequency. Thus, soil water content is determined by detecting changes in the operating frequency.

The FDR technique was employed for this research because previous research has shown that this type of probe can provide accurate soil moisture measurements (Huang et al. 2004). Continuous *in situ* real-time soil monitoring can be achieved by connecting the FDR unit to a data logger which tracks and stores the data. However, to ascertain the accuracy of the output from this unit, it is necessary to conduct a field-based test. With more soil moisture networks being established using the FDR sensors, it is imperative to affirm that the output from the sensors accurately reflects the absolute value of the soil moisture

content in the field. The first objective of this study was to test the accuracy of the default factory calibration by comparing it with observed volumetric soil moisture content across a range of different soils. The second objective was to derive field-based calibrations for the FDR probes based on soil textural class.

2.3 Methods

2.3.1 Hydra Probe Description and Laboratory Evaluation

The Steven's hydra probes were used in this study to measure soil water content. They are in widespread use for establishing soil moisture monitoring networks. For example, the Soil Climate Analysis Network of the Natural Resource Conservation Service uses the hydra probe to monitor soil moisture and it has proven to be robust under a variety of field conditions (Seyfried et al. 2005). The instrument has four 0.3 cm diameter stainless steel tines which are 5.7 cm long. These are arranged such that a central tine is surrounded by the other three in an equi-triangular position in a 3.0 cm diameter. The tines protrude from a 4.2 cm diameter cylindrical head which generates a 50-MHz signal, transmitted to the tines. The cylindrical measurement region or sensing volume, with length of 5.7 cm and a 3.0 cm diameter, is the soil between the stainless steel tines assembly. The tine assembly is often referred to as the wave guide and the probe signal is the average of the soil in the sensing volume (Stevens Water Monitoring System, Inc. 2008).

Prior to field deployment, the probes were tested in the laboratory to ensure that they provided consistent values under controlled conditions. A two-step assessment was carried out. First, the probes were submerged in distilled water. Typically, distilled water has a dielectric permittivity of about 80 and a range of 80 $\pm$ 5 is considered acceptable. All the probes were tested and their temperature-corrected dielectric constants were within the range of 78.1 – 81.7 which met the criteria for consistency between probes. As a second step, four of the probes were inserted into soils packed to known densities. This was done by adding water to air dried soils and mixing thoroughly. The moist soils of known weight were packed into containers with known volume to determine the bulk density of the soils. The probes were inserted into the moist soil to take readings and samples from each container were oven-dried for gravimetric analysis. Volumetric moisture content, derived from the product of the gravimetric water content and bulk density, was compared to the direct output from hydra probe reading. Four soil types were tested based on percent clay content and these were coarse, medium, fine and very fine soils which represent 0-20%, 20-40%, 40-60% and >60% clay content respectively. Each of these soil types was a mix of samples from fields across eastern and central Manitoba that falls within the textural classes defined. A laboratory calibration was developed for each soil type by plotting the observed volumetric water content against the dielectric permittivity of the soil.

The hydra probes output soil moisture ($m^3\ m^{-3}$), soil temperature (^oC and ^oF), real dielectric and imaginary constants (temperature-corrected and non-

temperature corrected) among other parameters. The temperature correction for the dielectric permittivity is often small.

2.3.2 Site Description

A weather station and four hydra probes were installed at each of the six monitoring sites in 2009. Three of these six fields were retained in 2010 with an additional 4 fields at new locations to give a total of seven fields in 2010 (Table 2.1). Two of the fields were about 30 m apart at the Treherne site with one field being annually cropped and the other a permanent grass area adjacent to the cropped field. Most of the sites were local farmers' fields except for the Kelburn, Oakville and Carman sites that were established for research purposes.

Table 2.1 Summary of field location, crop type and growing season (May-September) precipitation

Year	Field	Crop	GPS Coordinates	Precipitation (mm)
2009	Gladstone	Grass	**N**50.1420 **W**98.9497	277.4
	Kelburn	Oat	**N**49.6958 **W**97.1179	361.6
	Oakville	Canola	**N**49.9251 **W**98.0139	271.0
	Portage	Canola	**N**50.0040 **W**98.4652	284.5
	Treherne	Wheat	**N**49.6347 **W**98.6760	354.6
	Treherne	Grass	**N**49.6349 **W**98.6760	354.6
2010	Carman	Alfalfa	**N**49.4980 **W**98.0298	525.3
	Kelburn	Wheat	**N**49.6958 **W**97.1179	368.3
	Morden	Wheat	**N**49.2221 **W**98.2524	440.6
	Elm Creek	Canola	**N**49.7563 **W**98.0903	481.3
	Treherne	Canola	**N**49.6347 **W**98.6760	476.6
	Treherne	Grass	**N**49.6349 **W**98.6760	476.6
	Warren	Grass	**N**50.1225 **W**97.5968	611.6

(MAFRI, 2010).

For comparison, the climate normal precipitation (average precipitation for a 30-year period from 1971-2000) for south-eastern Manitoba during the growing period of May-September is 325 mm (Environment Canada, 2008). This showed a significant range of precipitation during the study.

2.3.3 Soil Classification

The Gladstone site was located in the Reinland series which consists of imperfectly drained, Gleyed Rego Black Chemozem soils developed on

moderately to strongly calcareous, stratified, deep, fluvial and lacustrine deposits. The Kelburn site was partly Osborne series (50%) and partly Glenmoor series (50%). Both series consist of poorly drained Rego Humic Gleysol soils, medium to high available water holding capacity. The Oakville site was located in the Willowbend Series. Like the Kelburn site, it consists of poorly drained Rego Humic Gleysols soils and has a high water table during the growing season. The Portage la Prairie site was located in the Pigeon Lake series which is a Gleyed Cumulic Regosol situated in a transition area between deep, loamy, recent fluvial deposits and clayey, lacustrine deposits. The series at the Treherne site was Tadpole which is a Rego Humic Gleysol, developed on poorly drained, strongly to very strongly calcareous, fine loamy, lacustrine sediments.

For the additional sites in 2010, the Carman plot was on Denham series which consists of moderately well drained Orthic Black soil, non-eroded, non-stony and non-saline soil with organic matter content and high natural fertility. In contrast, the Long Plain soil series dominated the Elm Creek site and is characterized by imperfectly drained gleyed Regosol soil developed on weakly to moderately calcareous, deep, sandy, deltaic deposits. The soil has low available water holding capacity and low organic matter content. The Morden site was 70% Darlingford series which consist of well drained Orthic Black Chernozem soils developed on moderately to strong calcareous, loamy mixed till deposits and have medium to moderately slow permeability. The remaining 30% was Ullrich series which consist of imperfectly drained Gleyed Black Chernozem. Lastly, the Warren site was 100% dominated by the Marquette soil series which

is an imperfectly drained Gleyed Rego Black soil developed on fine textured, moderately to strong calcareous deposits with slow permeability (MAFRI, 2006).

2.3.4 Hydra Probe Field Installation

At each field, four hydra probes were installed by digging a pit approximately 1 x 1 x 1 m and pushing the probes horizontally into one face of the pit at depths of 5, 20, 50 and 100 cm. The pits were dug near the edge of each field for accessibility but far enough into the field to provide representative values of soil moisture for the field without significant edge effects. At locations that had annual crops, the probes were installed as soon as possible after seeding. The surface 5 cm soil layer (and any vegetation) were carefully removed and set aside to be replaced on the surface when the pit was refilled. Each layer of soil; 5 – 20, 20 – 50, and 50 – 100 cm were removed, kept separately and replaced in the same stratum from which it was removed.

The profiles were dug to expose a face where the probes were inserted horizontally. A piece of plywood on the undisturbed soil surface adjacent to the pit face was used as the “soil surface” and a meter stick was used to measure down from the underside of the plywood to the four depths of interest. The hydra probes were inserted far enough to completely bury the tines in the soil to ensure firm contact. The cables for the four hydra probes were dropped down the pit wall to the bottom of the pit then run over to the opposite pit wall and back to the surface so that they did not come up out of the pit along the same wall in which

the probes were installed. This was done to avoid creating a channel where water could run directly down along the pit wall where the hydra probes were installed. The profile was then backfilled with the 50 – 100 cm soil that was removed being careful to pack the soil and to not jar or loosen the hydra probe. The other soil layers were backfilled and the surface 5 cm soil layer was carefully replaced. The 4 hydra probe cables were buried in a shallow (30 cm) trench back to the data logger so that tillage and field operations could proceed as normal leaving only about a 1 m^2 area to be avoided during fieldwork by the farmer.

2.3.5 Weather Stations and Meteorological Data

At each field, a weather station monitored rainfall (mm), air temperature (^oC), relative humidity and wind speed (m s^{-1}). Incoming solar radiation was also monitored at the Kelburn, Oakville, Portage, Gladstone, Carman, Morden and Elm Creek sites. All data were taken on hourly and daily time-steps. Rainfall was measured with a calibrated tipping bucket rain gauge and any gap in weather data was filled using observations from the nearest Environment Canada or Manitoba Agriculture Food and Rural Initiatives (MAFRI) meteorological station. MAFRI weather stations were used at the Gladstone, Treherne and Carman sites. Three Campbell Scientific weather stations and three WatchDog weather stations were used to monitor the other sites. The Campbell and watchdog weather stations were first set up adjacent to each other and cross-

validated in the spring before field deployment for about three weeks at the field research site at the University of Manitoba, Fort Garry Campus to ensure that all sensors provided comparable data.

Data from both the Campbell and WatchDog weather stations were downloaded on a weekly basis while data from the MAFRI stations were obtained via the internet.

2.3.6 Soil Moisture Measurement

Gravimetrically determined point measurements of soil moisture content were taken for calibration and validation purposes. During the 2009 growing season, gravimetric soil moisture samples were collected about five times at each site. This was increased to ten samples per site in 2010. The samples were taken about a meter away from the buried hydra probes using a Dutch auger. Depth ranges for the samples were 0-10cm, 15-25cm, 30-40cm, 45-55cm and 95-105cm. These depths, except the 30-40cm, were similar to the depths of the installed hydra probes; 5, 20, 50 and 100cm. The samples collected were weighed, oven-dried at 105 ^{0}C for 24 hours and weighed again to determine the gravimetric soil moisture content.

Soil bulk density determinations were used to convert the gravimetrically determined soil water content to observed volumetric water content (VWC).

$$\Theta_v = \Theta_g \text{ X } \rho_b \qquad (2.1)$$

Three bulk density determinations were done at all sites in both the 2009 and 2010 growing seasons. The mean value for each depth was determined and utilized in the volumetric soil moisture calculations. The flat bottom auger was used in 2009 and the Gidding soil probe was used in 2010 (Appendix A). Soil bulk density was calculated as the total mass of dry soil (M_{DS}) divided by the total volume (V_T) it occupies.

$$p_b = M_{DS} / V_T \qquad (2.2)$$

2.3.7 Calibration Procedure

To test the accuracy of the hydra probe, the VWC recorded by the probes was matched to the VWC (derived from gravimetric sampling). Volumetric water content is a linear function of the square root of real dielectric permittivity. Linear regression analysis was used to find the equation of best fit between the volumetric moisture content and the square root of the dielectric permittivity from the hydra probe,

$$\theta_V = a\,(\varepsilon_{TC})^{0.5} + b \qquad (2.3)$$

where θ_V is volumetric soil moisture content and ε_{TC} is the temperature corrected real dielectric permittivity. The values for the coefficients (a, b) are the slope and intercept respectively of the regression equation. Equation 2.3 was used for soils with less than 40% clay content. However, third order polynomials were utilized for soils with greater than 40% clay,

$$\theta_V = a + b(\varepsilon) + c(\varepsilon^2) + d(\varepsilon^3) \qquad (2.4)$$

where ε is the real dielectric permittivity and a, b, c and d are polynomial coefficients. The equations derived for each soil textural type were used to predict the volumetric water content on days when gravimetric samples were not taken and this was termed the 'observed water content'. The direct soil moisture output from the hydra probe based on the default factory calibration was termed the 'default water content'.

2.3.8 Statistical Procedure

To evaluate the performance of the FDR sensors in estimating soil moisture, the root mean square error (RMSE) was calculated as shown in Equation 2.5,

$$\mathrm{RMSE} = \left(\frac{\Sigma(fact_i - obs_i)^2}{n}\right)^{0.5} \qquad (2.5)$$

where *obs*. is the observed water content and *fact.* is the default factory water content, and *n* is the number of observations.

The mean bias error (MBE) was calculated to determine whether the default calibrations overestimate or underestimate soil water content. Positive values of MBE indicated overestimation, while negative values indicated underestimation. If the MBE is 0, it means that there is equal distribution of positive and negative differences,

$$MBE = \frac{1}{n}[\sum_{i=1}^{N}(Fact_i - Obs_i)] \quad (2.6)$$

where $Fact_i$ is the default factory water content on day *i* and Obs_i is the observed water content for that day. A paired student t-test at alpha level of 0.05 was conducted in order to assess whether the difference observed was significant.

The stability of the calibration equations were tested using the jack-knife full cross-test (Walker, 2007). A series of *n* prediction models M_n were developed using the observed data collected for each textural class from all fields. To test each model, the data were split into two parts; the first part included the data from *n-1*, and the second part had all the data *n*. The data from *n-1* were used for fitting a model $M_{(n-1)}$, which was developed using the same variables as the model M_n. The remaining data point was used for testing the model $M_{(n-1)}$. When this was completed for each n, it provided a full cross validation data set, where for each textural class, there was both an independent measured value and a predicted value based on the relationship determined independently from the other (Guo et al, 2010).

2.4 Results and Discussion

2.4.1 Laboratory Calibration

Soil Test Based on Textural Categories

For ease of comparison, various soil textural classes were binned into four groups which are coarse, medium, fine and very fine soil textures based on the percent clay content. These were defined as follows:

Coarse Texture: Less than 20% Clay Content (sand, loamy sand, sandy loam, and a fraction of silty loam and loam soils).

Medium Texture: 20-40% Clay Content (silty clay loam, clay loam, sandy clay loam and a fraction of silty loam and loam soils)

Fine Texture: 40-60% Clay Content (silty clay and clay soils)

Very Fine Texture: Greater than 60% Clay Content (Heavy Clay Soils)

The laboratory validation utilized one soil per textural class with each being tested at six different moisture contents and replicated 4 times. The mean of the four replicated hydra probe readings was used as the default factory value and this was compared to the observed value (from gravimetric analysis) for each data point. Table 2.2 shows the result of the hydra probes laboratory test. The default factory readings for soil moisture content were derived from the pre-set factory equation *0.109x–0.179* suggested by the manufacturer for loam soils, where *x* is the square root of non-temperature corrected real dielectric permittivity ($\sqrt{\varepsilon}$). All the hydra probes had this pre-set loam soil calibration by default from

the factory (Bellingham 2007) which was derived from the average of various soils tested. However, the manufacturer strongly recommended user-derived calibration coefficients when a higher level of accuracy is required for known soil textures.

Laboratory test results (Table 2.2, Figure 2.1) showed that the pre-set loam default calibration had the lowest RMSE in the medium soil category with a value of 0.006m^3 m^{-3} and the highest correlation coefficient of 0.999. This was not unexpected since the default parameters are for medium textured, loam soils. However, the factory parameters underestimated soil moisture in all other soil types as shown by the negative MBE. The results further showed an increase in the RMSE with increasing soil clay content from fine to very fine soil category.

There was no significant difference between the default calibration and the observed in both the coarse and the medium textured soils. However, both the fine and very fine textures showed a significant difference.

Table 2.2 Laboratory evaluation of hydra probes

Soil Category	*ε	*ε_{TC}	**Factory (m^3 m^{-3})	Observed (m^3 m^{-3})
	19.020	19.310	0.296	0.302
	20.340	20.660	0.313	0.321
Coarse	23.900	24.220	0.354	0.343
	26.380	26.770	0.381	0.400
	7.261	7.344	0.115	0.133
	7.662	7.758	0.123	0.132
Summary		**r^2: 0.992**	**RMSE: 0.013**	**MBE: -0.008**
			P(T<=t) one-tail	**0.065**
	22.090	22.390	0.333	0.329
	29.250	29.680	0.411	0.406
Medium	37.380	37.850	0.487	0.491
	36.260	36.720	0.477	0.466
	8.245	8.339	0.134	0.137
	8.421	8.523	0.137	0.136
Summary		**r^2: 0.999**	**RMSE: 0.006**	**MBE: 0.002**
			P(T<=t) one-tail	**0.178**
	29.199	29.574	0.410	0.426
	31.319	31.840	0.431	0.441
Fine	42.598	43.220	0.532	0.554
	44.470	45.042	0.548	0.589
	7.408	7.500	0.118	0.156
	7.321	7.415	0.116	0.155
Summary		**r^2: 0.997**	**RMSE: 0.030**	**MBE: -0.028**
			P(T<=t) one-tail	**0.002**
	26.253	26.620	0.379	0.404
	36.578	37.201	0.480	0.477
Very Fine	44.041	44.680	0.544	0.628
	55.502	56.280	0.633	0.651
	10.081	10.210	0.167	0.240
	10.524	10.651	0.175	0.241
Summary		**r^2: 0.968**	**RMSE: 0.054**	**MBE: -0.044**
			P(T<=t) one-tail	**0.014**

***** ε and ε_{TC} are dimensionless real and temperature corrected real dielectric permittivities.

****** Output from hydra probes using default factory calibration equation.

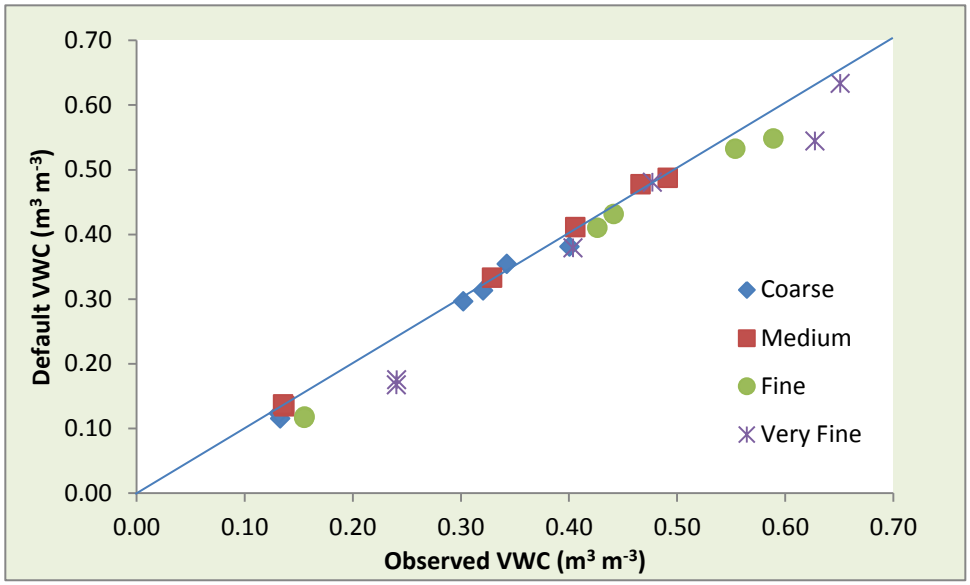

Figure 2.1 Laboratory test of hydra probe accuracy

Manufacturer's Suggested Polynomial Equation

The manufacturer proposed a polynomial equation for soils with high clay content. The polynomial equation as given by the manufacturer is:

$$\theta_V = 0.00324x^3 - 0.2464x^2 + 6.55x - 20.93 \qquad (2.7)$$

where x is the real dielectric permittivity (ε). The moisture contents using equation 2.7 were compared to those using the factory default linear equation. The results (Table 2.3) showed that the manufacturer-suggested clay equation gave better estimates in very fine textural class compared to the default loam equation. However, results obtained when the real dielectric constant was greater than 44.2 were not included because the polynomial equation gave unrealistically high readings at $\varepsilon > 44.2$.

The RMSE slightly increased from 0.028 m^3 m^{-3} to 0.030 m^3 m^{-3} in the fine textured soil but both the one and two tailed paired t-test showed that this difference was not significant. The manufacturer suggested polynomial equation for clay drastically reduced the RMSE in the very fine soil texture from 0.059 m^3 m^{-3} to 0.018 m^3 m^{-3} but showed significant difference only in the one tailed t-test. This improvement justifies the comparative advantage of using the manufacturer's suggested polynomial equation in heavy clay soils where user-specific calibration is unavailable. However, this comparative advantage may be undermined if values of $\varepsilon > 44.2$ are obtained.

Table 2.3 Comparing factory default (loam) output to manufacturer polynomial equation

Soil Category	ε	Observed (m^3 m^{-3})	Factory Default Equation (m^3 m^{-3})	Manufacturer Polynomial Equation (m^3 m^{-3})
Fine	29.199	0.426	0.410	0.410
	31.319	0.441	0.431	0.422
	42.598	0.554	0.532	0.617
	7.408	0.156	0.118	0.154
	7.321	0.155	0.116	0.151
			RMSE: 0.028	**RMSE: 0.030**
			P(T<=t) one-tail	**0.076**
Very Fine	26.253	0.404	0.379	0.399
	36.578	0.477	0.480	0.477
	44.041	0.628	0.544	0.666
	10.081	0.240	0.167	0.234
	10.524	0.241	0.175	0.245
			RMSE: 0.059	**RMSE: 0.018**
			P(T<=t) one-tail	**0.032**

ε is the dimensionless real dielectric permittivity.

Laboratory-Derived Calibration Equations

Laboratory calibration equations were derived for the four soil types. The slopes and intercepts of the regression equation between the $\sqrt{\varepsilon_{TC}}$ for coarse and medium soil textures, and the observed volumetric soil moisture were derived using linear regression analysis. However, third order polynomials were used for the relationship between the ε for fine and very fine soil textures, and the observed volumetric soil moisture content (Table 2.4). The types of equations for each texture category followed the conventions suggested by the manufacturer.

The linear equations derived for the coarse and medium textured soils were very comparable to the default factory equation of *0.109x–0.179*. However, the polynomials derived for the heavier textured soils were somewhat different from the manufacturer suggested polynomial equation (Equation 2.7).

Table 2.4 Laboratory Calibration Equations

Soil Type	n	Equation	R^2
Coarse	6	0.1056x - 0.157	0.99
Medium	6	0.1076x - 0.175	1.00
Fine	6	$0.0017x^3 - 0.1418x^2 + 4.5374x – 10.856$	1.00
Very Fine	6	$-0.0007x^3 + 0.0652x^2 - 0.7276x + 25.518$	0.98
Heavy*	12	$-0.00008x^3 + 0.0013x^2 + 1.211x + 8.742$	0.98

where x is $\sqrt{\varepsilon_{TC}}$ (square root of temperature corrected real dielectric permittivity) in coarse and medium, and **ε** (real dielectric permittivity) in fine and very fine soil texture.

* Combination of soils with >40% clay content i.e. fine and very fine soil texture.

The equations in Table 4 were further assessed using field observations of $\sqrt{\varepsilon}$ as discussed later in this chapter.

2.4.2 Hydra Probe Field Test

Bulk Density and Soil Texture

Table 2.5 shows the bulk density values used in converting the gravimetric soil moisture content to volumetric water content at each field-depth

Table 2.5 Site location with bulk density and textural class by depth

SITE	0-10cm	15-25cm	30-40cm* (g cm^{-3})	45-55cm	95-105cm
Oakville Canola 2009	1.20 **C**	1.39 **C**	1.14 **SiC**	1.31 **CL**	1.38 **SiL**
Portage Canola 2009	1.10 **SiCL**	1.40 **SiCL**	1.36 **SiCL**	1.45 **SiCL**	1.42 **C**
Gladstone Grass 2009	1.07 **SL**	1.34 **SL**	1.70 **LS**	1.78 **LS**	1.69 **S**
Kelburn Oat 2009	0.87 **HC**	1.20 **HC**	1.27 **HC**	1.40 **HC**	1.38 **HC**
Treherne Wheat 2009	1.18 **SL**	1.52 **SL**	1.29 **L**	1.55 **L**	1.64 **CL**
Treherne Grass 2009	0.84 **SL**	1.30 **SL**	1.28 **SL**	1.22 **SL**	1.69 **SCL**
Carman Alfalfa 2010	1.31 **CL**	1.47 **C**	1.39 **C**	1.60 **C**	1.54 **C**
ElmCreek Canola 2010	1.41 **S**	1.80 **S**	1.70 **S**	1.76 **S**	1.66 **LS**
Morden Wheat 2010	1.20 **CL**	1.40 **C**	1.32 **C**	1.45 **SiC**	1.39 **L**
Kelburn Wheat 2010	1.00 **HC**	1.20 **HC**	1.21 **HC**	1.40 **HC**	1.38 **HC**
Treherne Canola 2010	1.00 **SL**	1.53 **SL**	1.34 **L**	1.55 **L**	1.64 **CL**
Treherne Grass 2010	0.84 **SL**	1.30 **SL**	1.29 **SL**	1.22 **SL**	1.69 **SCL**
Warren Grass 2010	0.95 **HC**	1.08 **HC**	1.25 **HC**	1.25 **HC**	1.41 **HC**

Textural class keys: C = Clay, CL = Clay Loam, HC = Heavy Clay, SiC = Silty Clay, SL = Silty Loam, SiCL = Silty Clay Loam, L = Loam, LS = Loamy Sand, SL = Sandy Loam, SCL = Sandy Clay Loam, S = Sand.

* No hydra probes were installed at this depth but soil properties were determined.

Individual Hydra Probe Test

Results were obtained for twenty-four hydra probes for two growing seasons and four additional hydra probes in 2010 (Table 2.6) based on the factory default calibration. Twelve of these probes (two Treherne fields and Kelburn field) were left in place over the winter and were not re-installed in 2010. The other twelve hydra probes were at different fields in the 2009 and 2010 growing seasons. For data quality control, any soil moisture reading derived from the default factory calibration that were higher than the soil porosity were not used in data analysis. This was observed in some soils with very heavy clay which recorded soil moisture values between 0.75 and 1.1 $m^3\ m^{-3}$.

A comparison of the default factory readings of soil moisture to the gravimetrically-determined, volumetric field observed values showed large variations among field sites and depths. In 2009, there were five gravimetrically-derived soil moisture determinations taken at each site. The RMSE for individual probes based on five data points varied from 0.013 – 0.107 $m^3\ m^{-3}$ with a mean value of 0.043 $m^3\ m^{-3}$. In 2010, ten gravimetrically-derived soil moisture determinations were taken at each site and depth (Table 2.6). The RMSE for individual probes based on the ten data points varied from 0.027 – 0.174 $m^3\ m^{-3}$ with a mean value of 0.071 $m^3\ m^{-3}$. The larger variation in 2010 may be due to the change in fields.

A comparison of twelve hydra probes that were at the same field for both years showed a trend of increasing RMSE from the first year to the second year

in ten of the twelve hydra probes. This could be as a result of the freeze-thaw cycle that the hydra probes were subjected to as seasons change as well as the shrink-swell cycle of clay in heavy textured sites like Kelburn. The default hydra probe readings mostly overestimated the observed values as indicated by the positive MBE values.

Table 2.6 Hydra probe tests: A comparison of default soil moisture reading to field observations

Probe #	Depth	2009	RMSE*	MBE*	2010	RMSE**	MBE**
192783	100	Gladstone	0.030	0.009	Carman	0.070	0.062
192784	50	Gladstone	0.018	-0.005	Carman	0.174	0.167
192794	20	Gladstone	0.027	0.010	Carman	0.120	0.114
192787	5	Gladstone	0.020	0.012	Carman	0.074	-0.031
192781	100	Portage	0.071	0.070	Elm Creek	0.030	0.013
192788	50	Portage	0.052	0.052	Elm Creek	0.053	-0.040
192775	20	Portage	0.089	0.073	Elm Creek	0.036	-0.009
192789	5	Portage	0.062	0.037	Elm Creek	0.072	-0.062
192786	100	Treherne Wheat	0.013	-0.004	Treherne Canola	0.112	0.093
192791	50	Treherne Wheat	0.024	-0.001	Treherne Canola	0.061	0.047
192785	20	Treherne Wheat	0.038	0.037	Treherne Canola	0.054	0.005
192797	5	Treherne Wheat	0.030	-0.017	Treherne Canola	0.052	-0.015
192793	100	Treherne Grass	0.050	0.037	Treherne Grass	0.090	0.086
192795	50	Treherne Grass	0.016	0.001	Treherne Grass	0.043	-0.011
192796	20	Treherne Grass	0.029	0.012	Treherne Grass	0.028	0.011
192778	5	Treherne Grass	0.049	-0.037	Treherne Grass	0.028	-0.018
192798	100	Kelburn	0.032	0.019	Kelburn	0.081	0.054
192780	50	Kelburn	0.030	0.020	Kelburn	0.108	0.103
192779	20	Kelburn	0.033	0.017	Kelburn	0.053	0.041
192782	5	Kelburn	0.027	0.012	Kelburn	0.027	-0.016
192777	100	Oakville	0.042	0.030	Morden	0.074	0.006
192776	50	Oakville	0.095	0.092	Morden	0.036	0.021
192792	20	Oakville	0.107	0.093	Morden	0.124	0.113
192790	5	Oakville	0.057	0.023	Morden	0.038	-0.043
196721	100				Warren	***	
196720	50				Warren	***	
196719	20				Warren	0.115	0.111
196717	5				Warren	0.101	0.075

* Comparison based on five data points

** Comparison based on ten data points

*** FDR sensor reading with moisture content higher than the soil porosity

Soil Textural Category Test

In a bid to increase the number of calibration measurements and create a more robust comparison between the default factory reading and the observed data, the results were grouped into the same four textural classes defined in the laboratory procedure which was based on the percentage clay content. From table 2.5, coarse, medium, fine and very fine soil textural classes had 19, 12, 9 and 12 site-depths respectively. This was done to observe the accuracy of the default FDR reading in each textural category.

The results showed (Table 2.7) that the R^2 between the default factory hydra probe reading and the observed values decreased with increasing clay content except between the fine and very fine textures. The RMSE values increased with increasing clay content except between the fine and very fine textures. The default factory calibration slightly underestimated soil moisture for the coarse texture but overestimated it for the other soil categories. All the textural classes showed that the default calibrations were significantly different from the observed at $\alpha = 0.05$.

Table 2.7 Descriptive Analysis for each soil texture category.

	Coarse	*Medium*	*Fine*	*Very Fine*
N	131	76	60	59
RMSE	0.041	0.069	0.099	0.075
MBE	-0.007	0.045	0.081	0.049
P(T<=t) one-tail	0.02	3.0E-08	8.5E-18	5.3E-10
R^2	0.83	0.58	0.38	0.49

The R^2 values were higher in the laboratory evaluation and the RMSE values were lower, which is expected under controlled conditions in the laboratory. The factory default parameters, in general, overestimated soil moisture content especially in soils with 40% clay or higher when measured in field conditions.

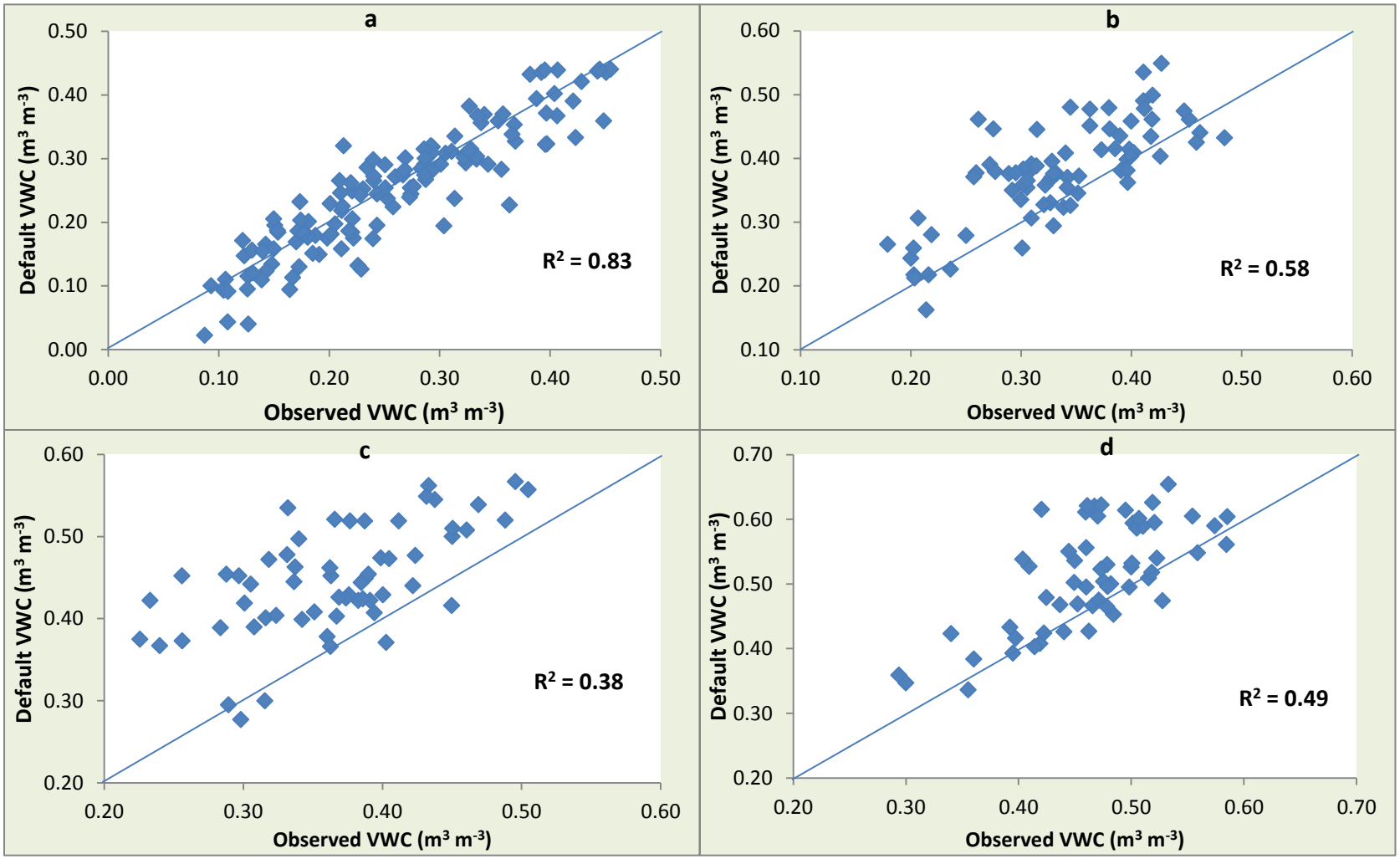
a
Default VWC (m³ m⁻³)
Observed VWC (m³ m⁻³)
R² = 0.83
0.00
0.10
0.20
0.30
0.40
0.50
b
Default VWC (m³ m⁻³)
Observed VWC (m³ m⁻³)
R² = 0.58
0.10
0.20
0.30
0.40
0.50
0.60
c
Default VWC (m³ m⁻³)
Observed VWC (m³ m⁻³)
R² = 0.38
0.20
0.30
0.40
0.50
0.60
d
Default VWC (m³ m⁻³)
Observed VWC (m³ m⁻³)
R² = 0.49
0.20
0.30
0.40
0.50
0.60
0.70

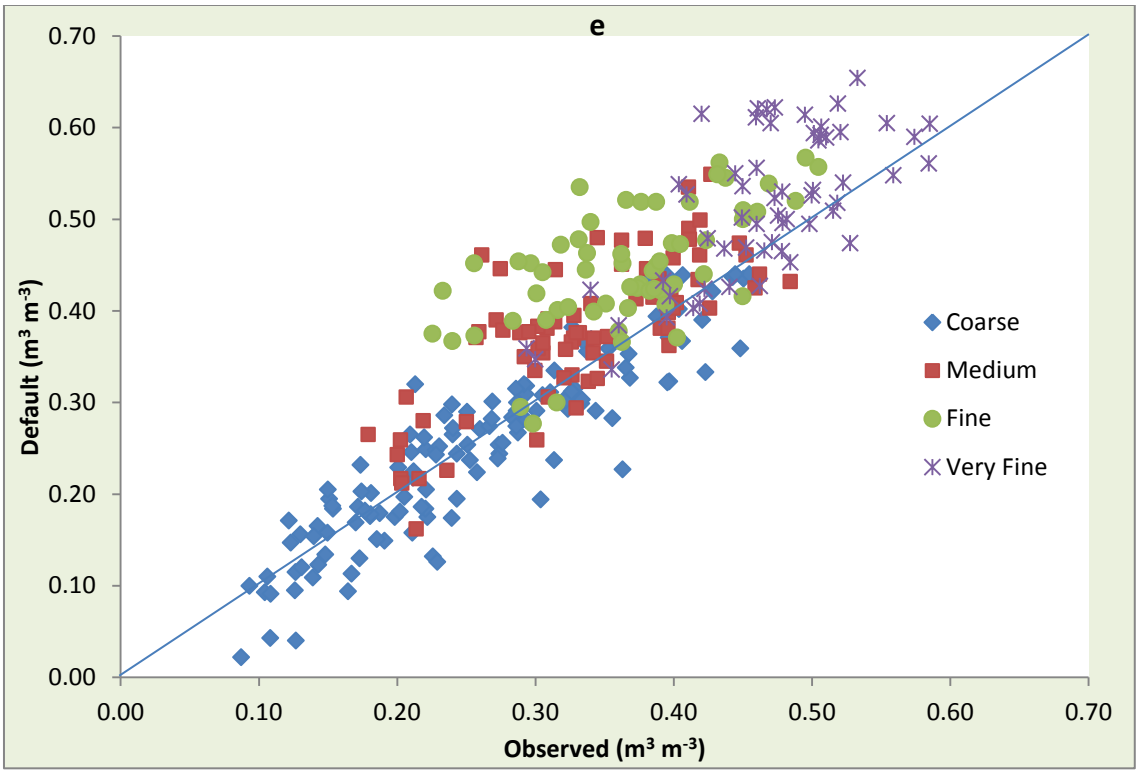

Figure 2.2 1:1 Comparison of observed moisture content and hydra probe default factory moisture content for (a) coarse; (b) medium; (c) fine; (d) very fine soil texture and (e) Combination of all points.

As expected, volumetric water content was generally higher as clay content increased from coarse soil type to very fine. Figure 2.2 c and d show significant scatter and mostly overestimated soil moisture values. Thus, the two textural groups, fine and very fine, were combined into one group called 'heavy' in subsequent analysis to give more calibration points for soils with high clay content (> 40%).

Field-Derived Calibration Equations

For coarse and medium textural categories, linear regression analysis was used to find the equation of best fit between the observed volumetric moisture content and the square root of the temperature corrected dielectric permittivity from the hydra probe. However, third order polynomials were derived for the heavy textural class from the non-temperature corrected real dielectric permittivity. This is consistent with the equation format suggested by the manufacturer for calibration in soils with high clay content (Equation 2.7). The equations derived (Table 2.8) were needed to predict the volumetric water content on days when gravimetric samples were not taken.

Table 2.8 Field calibration equations for coarse, medium and heavy soil textures.

Category	N	Equation	R^2
Coarse	131	0.09704x - 0.12478	0.83
Medium	76	0.07642x - 0.05692	0.57
Heavy	119	$-0.0007x^3 + 0.0725x^2 – 1.64x + 39.39$	0.56

where x is $\sqrt{\varepsilon_{TC}}$ (square root of temperature corrected real dielectric permittivity) in coarse and medium textures, and ε (real dielectric permittivity) in heavy texture.

The correlation coefficient in the combined heavy texture was improved to 0.56 compared to the R^2 of 0.38 and 0.49 of the individual fine and very fine texture respectively. However, using the third order polynomial decreased the

observed soil moisture content when the ε reached a maximum threshold value. This capped the observed values from the polynomial equation to a maximum of $0.52 m^3 m^{-3}$. In reality, soil moisture content in clay soils can be greater than this value. Thus, a linear equation should be used above the threshold value of ε = 50.0 (Figure 2.3c).

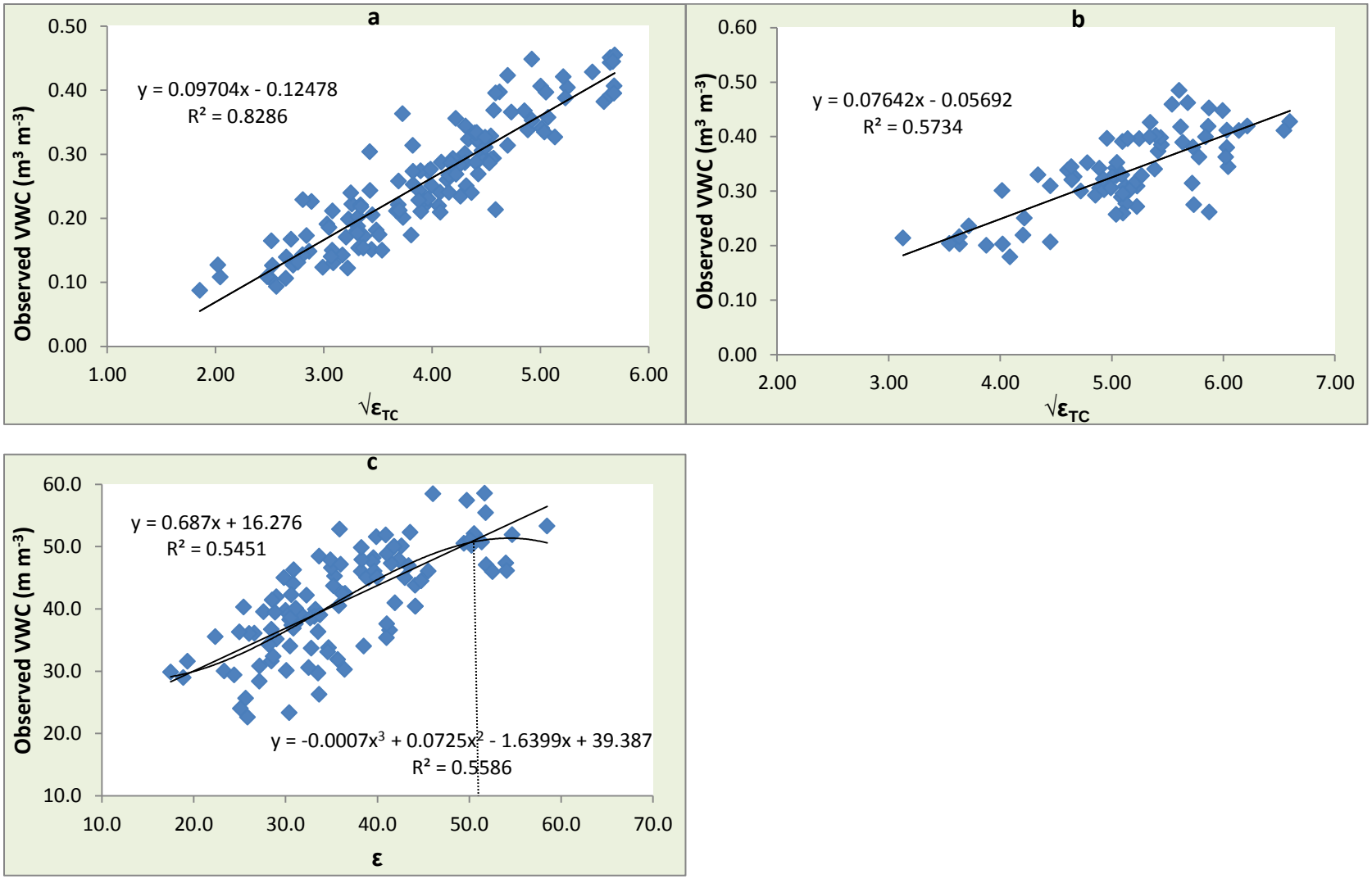

Figure 2.3 Field Calibration Plots . a – c represents coarse, medium and heavy soil textures respectively with plot c showing both linear and polynomial trendlines.

Field Calibration Equation Test

The stability of the field derived calibration equations were tested using the jack- knife full cross-test (Walker, 2007) with seventy five observed data points for each textural class. The total number of cross-calibration points (n-1) was limited to seventy-five for all soil texture group based on the smallest textural class – medium texture to provide similar basis for equation stability testing. Table 2.9 shows a comparison between the results obtained from field derived equations and field-observed values. A general trend of increasing RMSE and decreasing R^2 as the clay content increases was obvious across the categories. In coarse texture which had the highest R^2 value of 0.88, the field-derived calibration equation result slightly under-estimated the observed moisture content with a MBE of -0.002 and a RMSE of 0.037m^3 m^{-3}. Medium texture had equal magnitude but positive value of MBE which indicates a slight over estimation with a RMSE of 0.052m^3 m^{-3}. The heavy texture with the highest RMSE of 0.058 and lowest MBE and R^2 of -0.041 and 0.40, respectively showed that the observed values were under-estimated by the polynomial equation used.

Table 2.9 Summary Statistics of Validation Test

	Coarse	*Medium*	*Heavy*
N	75	75	75
RMSE	0.037	0.052	0.058
MBE	-0.002	0.002	-0.041
r^2	0.88	0.56	0.40

Laboratory, Factory, Suggested and Field Calibration Comparison

Equations derived from the laboratory and field calibrations (Tables 2.4 and 2.8 respectively) as well as the default factory calibration and the manufacturer suggested equations were used to calculate soil moisture content from the dielectric permittivity readings and these were compared to the field-observed values (Table 2.10). The result showed that the field derived equation had the lowest RMSE in all the three categories. Soils in the coarse and medium textural classes were close to loam texture, so the default equation doubled as the manufacturer suggested equation. However, the suggested clay equation highly overestimated soil moisture content for soils in the heavy texture class with a MBE of 0.149 and a RMSE of 0.253. This was due to the unrealistic high values derived from the third order polynomial when $\varepsilon > 44.2$. There was a significant reduction in both the RMSE and MBE of the suggested equation when $\varepsilon > 44.2$ values were excluded from the analysis. All the equations showed a progressive increase in RMSE as the clay content increased from coarse to heavy texture soils.

The time series (Figure 2.4) is shown for the 5 cm depth at four fields with each of the textural groups being represented. All three calibration equations had very good correlation at Gladstone, a coarse textured soil (Figure 2.4a) though they slightly overestimated observed soil moisture. This was typical of all fields with < 20% clay content. However, Carman (Figure 2.4b), representing fields with 20-40% clay content showed that both the default and laboratory calibrations were in close agreement and the field calibration underestimated the

observed soil moisture content at high values. Results from Portage and Kelburn (Figures 2.4 c and d, respectively) showed that the default and laboratory derived calibration equations consistently overestimated observed soil water content at peaks in the fine and very fine textured soils.

Seyfried et al (2005) compared the average difference between individual soil calibrations and multi-soil calibration equations using Time Domain Reflectometry probes. They found that clay soils had the highest difference averaging at 0.064 $m^3 m^{-3}$ compared to 0.037 $m^3 m^{-3}$ and 0.033 $m^3 m^{-3}$ for sand and silt respectively. In another experiment, Seyfried and Murdock (2004) evaluated three calibration equations supplied by the manufacturer in terms of the average difference between the measured and instrument-derived estimate for volumetric water content. They found that “the clay curve was the worst overall for every soil, the degree of fit was poor and the shape of the curve was unrealistic”. The difference for clay was as high as 0.125 $m^3 m^{-3}$ at one of the sites.

Table 2.10 Comparing Laboratory, Factory, Suggested and Field Calibrations

		Coarse N=134	*Medium N=79*	*Heavy N=110 (91)**
Default Equation	RMSE	0.040	0.072	0.084 (0.081)
	MBE	-0.007	0.038	0.061 (0.056)
Polynomial Equation	RMSE	-	-	0.253 (0.102)
	MBE			0.149 (0.074)
Laboratory Equation	RMSE	0.039	0.070	0.106 (0.101)
	MBE	0.001	0.035	0.088 (0.082)
Field Equation	RMSE	0.038	0.051	0.054 (0.056)
	MBE	-0.001	-0.004	0.002 (0.003)

* Values in bracket shows the result obtained when ε > 44.2 were excluded from the analysis.

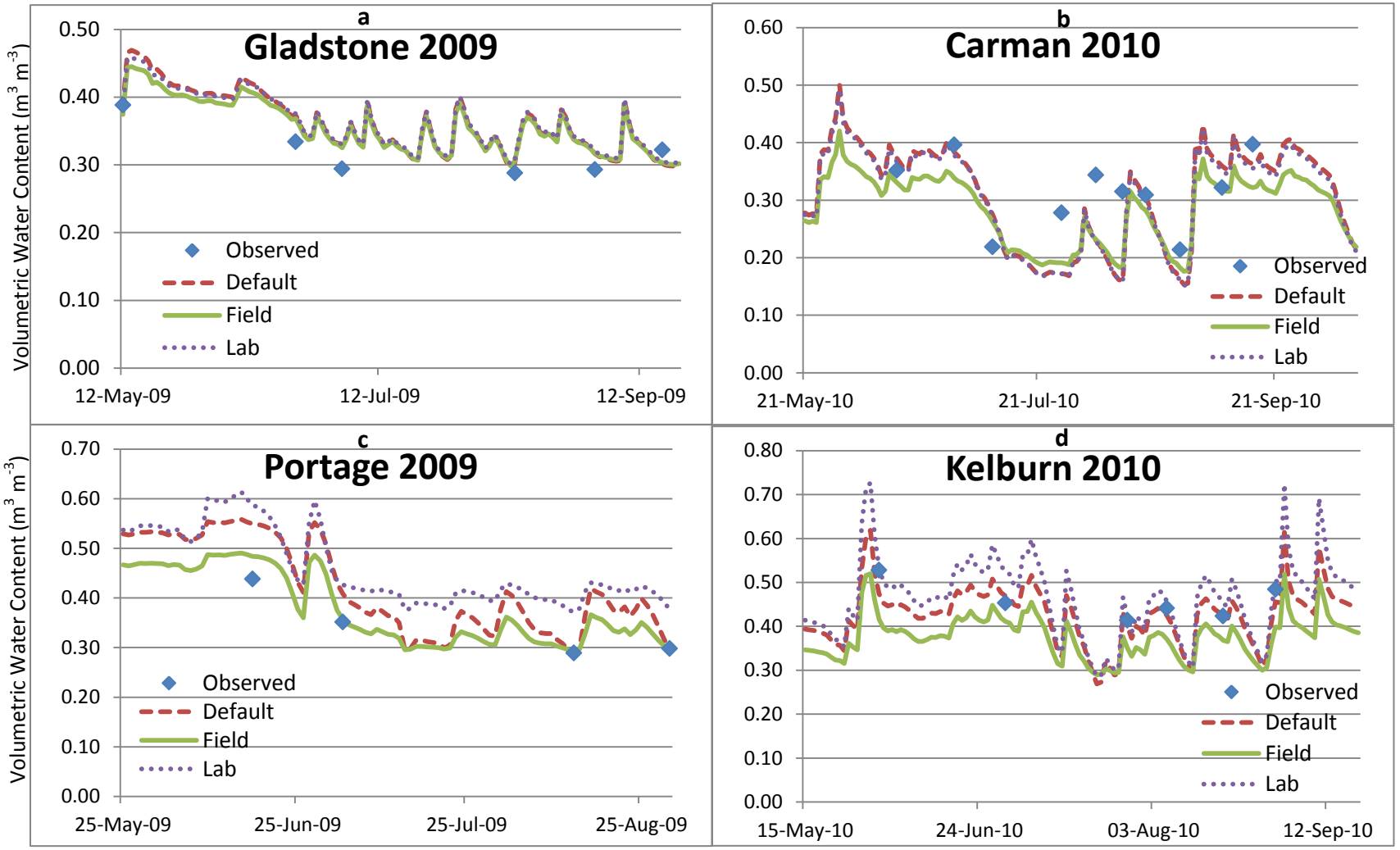

Figure 2.4 Time-series comparing the moisture content derived from the default factory, field and laboratory calibrations to field observed values at representative fields for each texture category at 5cm depth.

2.4.3 Limitations

Efforts were concentrated at minimizing errors in field calibration of the FDR sensors; however, uncertainty abounds especially in *in-situ* determination of soil bulk density. The observed field volumetric soil moisture was derived from the product of the soil bulk density and the gravimetric water content. Thus, errors in the bulk density determination especially at lower depths in the soil profile have an effect on the error of observed moisture content. The difficulty with bulk density determination at depth and its impact on volumetric soil moisture determination has been reported in previous research (Huang et al. 2004).

Another challenge is the spatial variability of soil since samples used for the gravimetric analysis differ from the actual soils in contact with the hydra probes. Soil samples used for the gravimetric analysis were taken about one meter from the buried sensors. The sensing volume of the FDR sensor, which is the soil that is close to the stainless steel prongs, is 5.7cm by length and 3.0cm diameter. It is therefore reasonable to assume that the soil moisture content of the soil in contact with the probes might be slightly different than that in soil extracted for the gravimetrically determined field observation. This is in contrast to the laboratory procedure in which the soil used for observed analysis was in direct contact with the probe.

2.5 Conclusion

This study showed that all the hydra probes were within the acceptable range when tested in water. The laboratory calibration was in close agreement with the manufacturer's equations, which shows repeatability for soil moisture measurement with the hydra probes in a controlled environment. However, the default factory parameters require adjustment before field-use, especially if deployed for use in fine textured soils. Though limitations abound due to the complex nature and spatial variation of field sampling as well as bulk density determination at depths, the need for field-based calibration of the FDR sensors especially in soils with high clay content is imperative since greater deviation of the hydra probe volumetric moisture content was observed with increasing clay content. For soils with less than 20% clay content, the default calibration seemed to suffice. The shrink-swell cycles of clay in response to water content most likely played a huge factor that affects hydra probes installed on such fields. Seyfried et al. (2005) reported that the weak relationship in soils with high clay content may be explained by the highly variable electrical properties of different clay minerals because dielectric loss is affected by clay properties such as surface area and CEC that are associated with different clay types. When user-specific field calibration is not determined, the manufacturer's suggested polynomial equation is preferred in clay-rich soils rather than the default factory calibration which is more accurate for loam textures. However, the polynomial equation should be capped at a dielectric permittivity maximum value of 44.2.

2.6 References

Bellingham, K. 2007. The Stevens Hydra Probe Inorganic Soil Calibrations. Stevens Water Monitoring Systems, Inc. [Online] Available: http://www.stevenswater.com/catalog/products/soil_sensors/datasheet/The%20Stevens%20Hydra%20Probe%20Inorganic%20Soil%20Calibrations.pdf [2011 May 5]

Brady, N.C and Weil, R.R. 1999. The Nature and Properties of Soils. (12th edition). Prentice-Hall Inc.

Briggs, L.J. 1897. The mechanics of soil moisture. USDA Bureau of Soils Bull. 10. U.S. Gov. Print. Office, Washington, DC.

Environment Canada. 2008. National Climate Data and Information Center. [Online] Available: http://climate.weatheroffice.gc.ca/climate_normals/stnselect_e.html [2010 December 27]

Guo, X.W., Fernando, W.G.D., Bullock, P. and Sapirstein, H. 2010. Quantifying cropping practices in relation to inoculum levels of *Fusarium graminearum* on crop stubble. Plant Pathology. **59:**1107-1113

Hook, W.R. and Livingston, N.J. 1996. Errors in converting time domain reflectometry measurements of propagation velocity to estimates of soil water content. Soil Sci. Soc. Am. J. **60:**35–41.

Huang, Q., Akinremi, O.O., Sri Ranjan, R. and Bullock, P.R. 2004. Laboratory and field evaluation of five soil water sensors. Can. J. Soil Sci. **84:**431-438.

Landa, E.R. and Nimmo, J.R. 2003. Soil History- The Life and Scientific Contributions of Lyman J. Briggs. Soil Sci. Soc. Am. J. **67:**681-693.

Lin, C.P. 2003. Frequency domain versus travel time analyses of TDR waveforms for soil moisture measurements. Soil Sci. Soc. Am. J. **67:**720–729.

MAFRI. 2006. Soil Survey Unit of the Agri-Environment Branch, Manitoba Agriculture, Food and Rural Initiatives, 362 Ellis Building, University of Manitoba, Winnipeg.

MAFRI. 2010. Manitoba Ag-Weather Program. [Online] Available: http://tgs.gov.mb.ca/climate/Default.aspx [2010 December 27]

Robinson, D.A., Campbell, C.S., Hopmans, J.W., Hornbuckle, B.K., Jones, S.B., Knight, R., Ogden, F., Selker, J. and Wendroth, O. 2008. Soil moisture measurements for ecological and hydrological watershed scale observatories: a review. Vadose Zone J. **7:**358–389.

Robock, A., Vinnikov, K.Y., Srinivasan, G., Entin, J.K., Hollinger, S.E., Speranskaya, N.A., Liu, S. and Namkhai, A. 2000. The global soil moisture data bank. B. Am. Meteorol. Soc. **81** (6), 1281–1299.

Seneviratne, S.I., Corti, T., Davin, E.L., Hirschi, M., Jaeger, E.B., Lehner, I., Orlowsky, B. and Teuling, A.J. 2010. Investigating soil moisture-climate interactions in a changing climate: A review. Earth-Science Reviews **99:**125-161.

Seyfried, M.S., Grant, L.E., Du, E. and Humes, K. 2005. Dielectric Loss and Calibration of the Hydra Probe Soil Water Sensor. Vadose Zone Journal. **4:**1070-1079.

Seyfried, M.S. and Murdock, M.D. 2004. Measurement of Soil Water Content with a 50-MHz Soil Dielectric Sensor. Soil Sci. Soc. Am. J. **68:**394-403.

Stevens Water Monitoring System, Inc. 2008. The Hydra Probe Soil Sensor. Comprehensive Stevens Hydra Probe User's Manual. [Online] Available: http://www.stevenswater.com/catalog/products/soil_sensors/manual/Hydra%20Probe%20Manual%2092915%20June%202007.pdf [2011 May 5]

Topp, G.C. 2003. State of the art of measuring soil water content. Hydrological Processes. **17:** 2993–2996

Walker, D.A. 2007. Estimation prediction accuracy: a comparison of proportional bias. Multiple Linear Regression Viewpoints. **33**: 32–38.

Walker, J.P., Willgoose, G.R. and Kalma, J.D. 2004. In situ measurement of soil moisture: a comparison of techniques. Journal of Hydrology. **293:**85-99

3 Comparison of Evapotranspiration Methods

3.1 Abstract

Seasonal excess or deficit of soil moisture has been found to be one of the most limiting factors to agricultural production in the prairies. To aid our understanding of the various complex processes involved in soil water content fluctuation especially, the removal of water from soil and plant surfaces, indirect methods have been employed. The gaseous nature of water vapour makes direct measurements a daunting task. VSMB, a model that simulates soil moisture, uses solar radiation from Hargreaves' equation and the Priestley-Taylor (PT) equation to estimate evapotranspiration (ET_o). These are important inputs in the model. Access to direct solar radiation data from pyranometers as well as additional meteorological data including humidity and wind speed allow for the improved estimation of evapotranspiration using the Penman-Monteith FAO-56 (PM) method. Therefore, the VSMB was modified to take advantage of improved meteorological data access. Comparisons were made between the observed solar radiation and the Hargreaves equation. Overall, the Hargreaves equation overestimated solar radiation with a root mean square error of 5.0MJ m^{-2} day^{-1} and a positive mean bias error of 1.5. The Hargreaves estimates were statistically different from the observed pyranometer data. However, on non-rainy days, no statistical difference was observed. The PM was also tested against the PT for ET_o and it was observed that the PT underestimated PM ET_o with a root mean square error of 0.88mm day^{-1} and a negative mean bias error of -0.42.

3.2 Introduction

The necessity for efficient water management in improving crop production is important for agricultural producers. Timely knowledge of soil moisture fluctuations help farmers in irrigation scheduling, especially, since soil moisture content at the rooting depth of most prairie soils is rarely sufficient to meet evapotranspirative demands in a typical growing season. Shepherd and McGinn (2003) reported that the historic mean daily soil moisture content is 82 mm in the upper 120 cm of soil for Alberta, 47 mm for Saskatchewan and 76 mm for Manitoba. They observed that the low value for Saskatchewan coincides with the lower annual precipitation of 395 mm in Saskatchewan compared to 482 mm for Alberta and 486 mm for Manitoba (Shepherd and McGinn, 2003). Some farmers monitor rainfall events on their farms using various types of rain gauges. This gives them an idea of the quantity of rainfall over a given period of time. Although this is useful information, it is more meaningful to determine its influence on soil moisture content.

Soil moisture monitoring has evolved over the years with the use of various soil moisture monitoring sensors which work on different principles targeted at estimating soil water content. These sensors relate specific soil properties to the amount of water in the soil. However, the high cost of these sensors and sometimes, the level of expertise needed for their installation have limited their use in many areas. To fill this gap, models are employed. Models are a simplification of real world processes which help to improve our understanding of the element being simulated and to make predictions about the

future based on information about all the phenomena related to the situation to be modeled. Models are able to overcome the shortcomings of point data from direct soil moisture measurement which do not integrate these measurements over space and time as is often required in many agronomic applications (Akinremi and McGinn 1996; Baier and Robertson 1966; De Jong 1981). Modeling often involves the integration of knowledge from various fields of science to solve a problem and it has been widely used for many purposes. The increase in the number of scientific papers on modeling in the Agricultural and Forest Meteorology journal from 1.2% to 19.4% within a-34 year span from 1964-1998 (Monteith, 2000), attests to the fact that modeling has evolved to become a very useful tool in agrometeorology.

One of the basic strategies for modeling soil moisture is the water balance approach. Like every storage system, the amount of water held in the soil is dependent on water input and output pathways.

$$\Delta SM = P + I + CR - ET - DD - RO - \Delta SS \qquad (3.1)$$

where:

ΔSM = Change in soil moisture
P = Precipitation
I = Irrigation
CR = Capillary Rise
ET = Evapotranspiration
DD = Deep Drainage
RO = Runoff
ΔSS = Change in the sub-surface flow

However, a simplified water balance model takes into account, the main input and output pathways which are precipitation and evapotranspiration respectively. It is assumed that the influence of other factors is negligible, which can be a reasonable assumption during the growing season in a semi-arid climate, such as western Canada, where deep drainage and runoff do not frequently occur.

$$\Delta SM = P - ET \qquad (3.2)$$

Precipitation during the growing season occurs mostly as rainfall which is directly measured using rain gauges. However, the loss of water from a soil-plant surface is not easily measured. The first objective of this study was to compare solar radiation data from direct measurement using the pyranometer to results from Hargreaves equation. The second objective was to compare the Priestley-Taylor (PT) ET_o equation to the Penman-Monteith ET_o.

3.3 Methods

3.3.1 Reference Evapotranspiration

Introduction and Development

Evapotranspiration is the combined process of water transfer to the atmosphere by evaporation and transpiration in a soil-plant system. It is a major pathway for water loss from the earth surface in the hydrologic cycle. Its

gaseous nature makes it difficult to directly and accurately quantify. One of the early methods used was pan-evaporation which gauges water loss from open water of known volume (or depth) held in a pan container.

H.L Penman (1948) observed that evaporation from bare soil involves complex soil factors as well as atmospheric conditions. Transpiration studies further add to these important physical and biological features. A plant's root system can draw on moisture throughout a considerable depth of soil, its aerial parts permit vapour transfer throughout a considerable thickness of air, and its photo-sensitive stomatal mechanism restricts this transfer to the hours of daylight. Penman's study was restricted to consideration of the early stages that would arise after thorough wetting of the soil when soil type, crop type and root range are of little importance but mainly dependent on environmental drivers, a term referred to as Potential Evaporation.

$$\lambda E = \frac{\Delta(R_n - G) + (\gamma \lambda E_a)}{(\Delta + \gamma)} \qquad (3.3)$$

where:

$\boldsymbol{\lambda E}$ evaporative latent heat flux [$MJm^{-2}day^{-1}$]

$\boldsymbol{R_n}$ net radiation at crop surface [$MJ\ m^{-2}\ day^{-1}$]

$\boldsymbol{\lambda}$ latent heat of vaporization [$MJ\ kg^{-1}$]

$\boldsymbol{G}$ soil heat flux density [$MJ\ m^{-2}\ day^{-1}$]

Δ slope of vapour pressure curve [$kPa\ °C^{-1}$]

$\boldsymbol{\gamma}$ psychrometric constant [$kPa\ °C^{-1}$]

$\boldsymbol{E_a}$ vapour transport flux = $W_f\ (e_s - e_a)$ [$mm\ day^{-1}$] with W_f being a wind function.

Based on the requirements that must be met to permit continued evaporation, Penman proposed an equation that combines the supply of energy which provides latent heat of vaporization with a mechanism to remove the vapour from the surface (Equation 3.3). However, routine weather data requirements like wind speed, which were not widely available at the time, as well as the necessity for tedious computations without computers, made most users prefer simpler evapotranspiration estimation methods such as the Blaney-Criddle and Thornthwaite (Howell and Evett, 2004).

Thornthwaite's original method (Thornthwaite, 1948) used average temperature for a given day or period (*T*), climatological normal annual temperature (T_a) and the photoperiod (maximum number of sunshine hours, *N*) as inputs. The last two inputs can be obtained from tabular indexes and this method is not recommended for use in areas that are not climatically similar to the east-central USA, where it was developed (Jensen, 1973). The Blaney-Criddle method, a simpler approach estimates ET using the formula:

$$ET_o = p\,(0.46T_{mean} + 8) \qquad (3.4)$$

where

ET_o = ET (mm/day) as an average for a period of one month

T_{mean} = Mean daily temperature (^oC)

p = Mean daily percentage of annual daytime hours

This method, though simple, is not very accurate especially under extreme climatic conditions as it only provides a rough estimate. In windy, dry, sunny

areas, ET_o is underestimated up to about 60%, while in calm, humid, clouded areas, ET_o is overestimated up to about 40% (FAO, 1986). The need to have less tedious but more accurate methods of estimating ET_o led to the development of many other agro-meteorological equations, most of which are adapted to the climatic area where they were developed. Hargreaves and Samani (1985) estimated ET_o using only maximum, minimum and mean temperatures and extraterrestrial solar radiation using equation 3.11:

$$ET_o = 0.0023R_a (T_{max} - T_{min})^{0.5} (T_{mean} + 17.8) \qquad (3.5)$$

where R_a = Extraterrestrial solar radiation

These agrometeorological equations were tested against lysimeter readings, often used as the standard (Kashyap and Panda, 2001). Lysimeters are hydrologically isolated soil-plant system tanks that are installed to monitor soil moisture fluxes. More recently, the eddy covariance method has gained acceptance as a means for direct ET_o measurement. It measures the transfer of water vapour from a surface to the atmosphere by correlating fluctuations of vertical wind speed with fluctuations in atmospheric water vapour density.

The Penman Monteith (FAO-56)

The original Penman equation (Equation 3.3), though noted for its tedious computation, was also seen as having a solid basis for ET estimation. Most

modifications to this original method focused on the aerodynamic term. Priestley and Taylor (1972) simplified the original Penman equation by replacing the aerodynamic term with an empirical coefficient of 1.26 (Equation 3.6). However, this coefficient varies with different vegetation types, soil moisture conditions and strength of advection (Priestley and Taylor, 1972; Stannard, 1993; Suleiman and Hoogenboom, 2007; Sentelhas et al, 2010).

$$ETo = 1.26\ \frac{\Delta}{\Delta+\gamma}\left(\frac{Rn-G}{\lambda}\right) \qquad (3.6)$$

In 1965, Montheith suggested a canopy resistance term and a roughness length for vapour and for momentum (Kashyap and Panda, 2001). The bulk canopy resistance (r_s) describes the resistance of vapour flow through the transpiring crop and evaporating soil surface while the transfer of heat and water vapour from the evaporating surface to the air above the canopy is determined by the aerodynamic resistance (r_a) (Allen et al., 1998).

$$r_s = \frac{r_i}{LAI_{active}} \qquad (3.7)$$

where

r_s (bulk) surface resistance [s m^{-1}],

r_i bulk stomatal resistance of the well-illuminated leaf [s m^{-1}],

LAI_{active} active (sunlit) leaf area index [m^2 (leaf area) m^{-2} (soil surface)].

$$r_a = \frac{ln\left[\frac{z_m-d}{z_{om}}\right]ln\left[\frac{z_h-d}{z_{oh}}\right]}{k^2 u_z} \qquad (3.8)$$

where

r_a aerodynamic resistance [s m^{-1}],

z_m height of wind measurements [m],

z_h height of humidity measurements [m],

d zero plane displacement height [m],

z_{om} roughness length governing momentum transfer [m],

z_{oh} roughness length governing transfer of heat and vapour [m],

k von Karman's constant, 0.41,

u_z wind speed at height z [m s^{-1}].

The advancement in technology, introduction of computers and weather sensors that monitor key weather parameters in real-time has led to rapid changes in ET estimation. The Food and Agricultural Organization (FAO) developed technical papers to assist in the standardization and accuracy of ET estimation. One such paper, developed in 1977 was the FAO Irrigation and Drainage Paper No. 24 titled 'Crop Water Requirements' by Doorenbos and Pruitt (1977). The FAO Penman method, recommended by the FAO 24 paper was found to frequently overestimate ET_o while the other FAO recommended equations, showed variable adherence to the grass reference crop evapotranspiration.

Reviewing the FAO 24, Allen et al (1998) recommended the adoption of the Penman-Monteith combination method as a new standard for reference evapotranspiration (Equation 3.9) and advised on procedures for calculating the various parameters. The FAO Penman-Monteith method was developed by defining the reference crop as a hypothetical grass surface with an assumed

height of 0.12 m, with a surface resistance of 70 s m^{-1} and an albedo of 0.23, closely resembling the evaporation from an extensive surface of green grass of uniform height, actively growing and adequately watered. The method overcomes the shortcomings of the previous FAO Penman method and provides values that are more consistent with actual crop water use data worldwide. Furthermore, recommendations have been developed using the FAO Penman-Monteith method with limited climatic data, thereby largely eliminating the need for any other reference evapotranspiration methods and creating a consistent and transparent basis for a globally valid standard for crop water requirement calculations.

$$\lambda ET = \frac{\Delta(R_n - G) + \rho_a c_p \frac{(e_s - e_a)}{r_a}}{\Delta + \gamma\left(1 + \frac{r_s}{r_a}\right)} \qquad (3.9)$$

where R_n is the net radiation, G is the soil heat flux, $(e_s - e_a)$ represents the vapour pressure deficit of the air, ρ_a is the mean air density at constant pressure, c_p is the specific heat of the air, Δ represents the slope of the saturation vapour pressure temperature relationship, γ is the psychrometric constant, and r_s and r_a are the (bulk) surface and aerodynamic resistances.

From the original Penman-Monteith equation (Equation 3.9) and the equations of the surface resistance (Equation 3.7) and aerodynamic resistance (Equation 3.8), Allen et al. (1998) presented the FAO 56 Penman-Monteith method to estimate ET_o as:

$$ET_o = \frac{0.408\Delta(R_n - G) + \gamma \frac{900}{T+273} u_2 (e_s - e_a)}{\Delta + \gamma(1 + 0.34u_2)} \quad (3.10)$$

where

ET_o reference evapotranspiration [mm day^{-1}],
R_n net radiation at the crop surface [MJ m^{-2} day^{-1}],
G soil heat flux density [MJ m^{-2} day^{-1}],
T mean daily air temperature at 2 m height [°C],
u_2 wind speed at 2 m height [m s^{-1}],
e_s saturation vapour pressure [kPa],
e_a actual vapour pressure [kPa],
$e_s - e_a$ saturation vapour pressure deficit [kPa],
Δ slope vapour pressure curve [kPa $°C^{-1}$],
γ psychrometric constant [kPa $°C^{-1}$].

For the purpose of estimating daily ET_o, all the parameters above can be estimated from four basic weather measurements which are temperature, humidity, solar radiation and wind speed. Since the release of the FAO 56 Penman Montheith (FAO-56) method, many scientists have worked at validating this method under various conditions (shorter time-steps and when some data are not available) as well as its comparative advantage over previously used methods.

Kashyap and Panda (2001) evaluated ten climatological methods of estimating reference ET and compared the result with a weighing lysimeter. The climatological methods compared were: Penman, FAO-Penman, FAO-Corrected-

Penman, 1982-Kimberley-Penman, Penman-Monteith, Turc-Radiation, Priestley-Taylor, FAO-Radiation, Hargreaves and FAO-Blaney-Criddle.

Table 3.1 Comparison of various climatological ET_o methods (Kashyap and Panda 2001)

Rank	Estimation Method	Mean Deviation from Measured Values (%)	R MSE (mm day^{-1})
1	Penman-Monteith FAO 56	-1.36	0.080
2	Kimberly-Penman	-1.51	0.211
3	FAO-Penman	-3.60	0.234
4	Turc-Radiation	+2.72	0.260
5	FAO-Blaney-Criddle	+3.16	0.289
6	Priestley-Taylor	-6.28	0.316
7	Penman	+11.87	0.317
8	Hargreaves	+8.34	0.358
9	FAO-Radiation	+17.89	0.540
10	FAO-Corrected Penman	+22.32	0.756

The results presented in Table 3.1 show that the FAO 56 method had the lowest RMSE and mean deviation. Studies such as this and others (Pereira et al., 2002; Lopez-Urrea et al., 2006; Xing et al., 2008) have increased the level of confidence in using the FAO-56 method as a standard to which other methods are compared. Since the cost and labour involved in setting up a lysimeter is high, having a reliable basis of comparison is of great importance. This is not to assume that the FAO-56 ET_o is totally perfect but a RMSE of 0.080mm day^{-1} is

quite close to reality. In the past, the use of the FAO-56 ET_o has been limited due to data requirement and the complex computations. However, with an increasing number of automated weather stations and computer programs, these draw-backs have been surmounted.

The current version of the VSMB (VB_0) computes solar radiation data from Hargreaves equation given as:

$$R_s = 0.16(T_{max} - T_{min})^{0.5} R_a \quad (3.11)$$

where R_s is the incoming shortwave radiation (MJ m^{-2} d^{-1}), T_{max} and T_{min} are the daily maximum and minimum temperatures, R_a (MJ m^{-2} d^{-1}) is the extraterrestrial radiation obtained from solar constant, latitude and Julian day. However, with the increasing number of meteorological stations with pyranometers for measuring incoming solar radiation, the VSMB model was modified (VB_1) to read solar radiation data directly if provided. If not, the model uses equation 3.11 to compute it. The incoming solar radiation data is needed for the determination of the net radiation (R_n) parameter in equation 3.10. R_n computation by Allen et al. (1998) is given as:

$$R_n = R_{ns} - R_{nl} \quad (3.12)$$

$$R_{ns} = 0.77R_s \quad (3.13)$$

$$R_{nl} = \sigma\left[\frac{T_{maxK^4} + T_{minK^4}}{2}\right]\left(0.34 - 0.14\sqrt{e_a}\right)\left(1.35\frac{R_s}{R_{so}} - 0.35\right) \quad (3.14)$$

$$R_{so} = R_a[0.75 + (2 \times 10^{-5})z] \quad (3.15)$$

where

R_n net radiation [MJ m^{-2} day^{-1}],
R_{ns} net incoming shortwave radiation [MJ m^{-2} day^{-1}],
R_{nl} net outgoing longwave radiation [MJ m^{-2} day^{-1}],
R_a extraterrestrial solar radiation [MJ m^{-2} day^{-1}],
σ Stefan-Boltzmann constant [4.903 10^{-9} MJ K^{-4} m^{-2} day^{-1}],
T_{maxK} maximum absolute temperature during 24-hour period [K = °C + 273.16],
T_{minK} minimum absolute temperature during 24-hour period [K = °C + 273.16],
e_a actual vapour pressure [kPa],
R_s/R_{so} relative shortwave radiation (limited to ≤ 1.0),
R_s measured or calculated (equation 3.15) solar radiation [MJ m^{-2} day^{-1}],
R_{so} calculated (equation 3.19) clear-sky radiation [MJ m^{-2} day^{-1}].
z station elevation above sea level (m).

The net radiation calculation in equation 3.12 replaces the one currently used by the VSMB (equation 3.16) which provides an easy estimate of net radiation (R_n, W m^{-2}) without actual radiation data.

$$R_n = 0.63R_s - 40 \qquad (3.16)$$

These changes in net radiation computation are expected to improve reference evapotranspiration estimates. Furthermore, the Priestley-Taylor (PT) equation (Equation 3.6) currently used to estimate ET_o was replaced with the FAO 56 equation (equation 3.10) based on studies (Table 3.1) which affirm that the FAO-56 method gives better ET_o estimates.

VB_0 utilizes the minimum and maximum daily temperature, and precipitation. However, to accommodate the changes made, additional weather

data were added to the VSMB weather input file. These are minimum and maximum humidity, wind speed and solar radiation data.

3.3.2 Statistical Procedure

To evaluate the performance of the Hargreaves equation in estimating solar radiation, the root mean square error (RMSE) was calculated as shown in Equation 3.17.

$$\mathrm{RMSE} = \left(\frac{\Sigma(Harg_i - Obs_i)^2}{n}\right)^{0.5} \qquad (3.17)$$

where Obs_i is the observed solar radiation reading from the pyranometer on day *i* and $Harg_i$ is the solar radiation calculated from the Hargreaves equation on day *i*, and *n* is the number of observations.

The mean bias error (MBE) was calculated to determine whether the Hargreaves equation overestimates or underestimates solar radiation. Positive values of MBE indicated overestimation, while negative values indicated underestimation. If the MBE is 0, it means that there is equal distribution of positive and negative differences.

$$MBE = \frac{1}{n}\left[\sum_{i=1}^{\mathrm{N}}(Harg_i - Obs_i)\right] \qquad (3.18)$$

The percentage mean deviation from measured values was also determined to estimate in percentage terms, the average deviation of the Hargreaves-derived result from the observed pyranometer values.

$$\%MD = \frac{1}{n}\left[\sum_{i=1}^{N}\left(\frac{Harg_i - Obs_i}{Obs_i} * 100\right)\right] \qquad (3.19)$$

A paired student t-test at alpha level of 0.05 was conducted in order to assess whether the values from the Hargreaves equation were significantly different from the observed pyranometer values. These statistics were also used to compare results from daily PT ET_o to values from the Penman Monteith FAO-56 ET_o.

3.4 Results and Discussion

3.4.1 Observed Solar Radiation versus the Hargreaves Model

The incoming solar radiation data taken directly using the pyranometer was compared to simulated results using Hargreaves equation (equation 3.11). The current version of the VSMB (VB_0) uses this equation. Though automated solar radiation sensors are now more widely in use, many radiation-based models still use the Hargreaves method. The daily incoming solar radiation data collected at seven sites with a pyranometer installed were compared to solar radiation data generated from the Hargreaves equation for the 2009 and 2010 growing season. Overall, the Hargreaves equation captured the trend in daily values correctly. However, it overestimated solar radiation at low observed values and underestimated it at higher values. The equation was not able to capture these extremes (Figure 3.1).

Pooling the data from all sites for both 2009 and 2010, the root mean square error was 5.0 MJ m^{-2} day^{-1} and the mean bias error was +1.5 which means that the Hargreaves equation overestimated solar radiation. The percentage mean deviation from observed value was 26.0%. The Hargreaves estimates were statistically different from the observed pyranometer data. However, on non-rainy days, no statistical difference was observed (Table 3.2). The RMSE was reduced to 3.9 MJ m^{-2} day^{-1} and a mean bias error of +0.02 which indicates a slight overestimation.

Table 3.2 Paired Two Sample t-test (Hargreaves vs Observed).

	All Days		Non-Rainy Days	
	Harg	*Obs*	*Harg*	*Obs*
Mean	20.36	18.87	21.71	21.69
Standard Deviation	4.44	6.94	16.25	28.65
Observations	646	646	397	397
Hypothesized Mean Difference	0		0	
Df	645		396	
t Stat	7.97		0.01	
P(T<=t) one-tail	3.61E-15		0.46	
t Critical one-tail	1.65		1.65	
P(T<=t) two-tail	7.21E-15		0.92	
t Critical two-tail	1.96		1.96	
α	0.05		0.05	

A review of the days with observed low solar radiation values from the pyranometer revealed that the low extremes mostly occurred on rainy days with high humidity (Figure 3.1). There is a possibility however, that condensation on the sensors' surface might have interfered with its ability to correctly read the incoming solar radiation on such days. Bubgee and Tanner (2001) observed that the flat surface castle design of the sensor head tends to trap water and cause the sensor to underestimate solar radiation values up to 20%. However, the pyranometers used for this study were the dome-surface design which helps to repel water and facilitates self-cleaning. Thus, the influence of rainfall on pyranometer reading is expected to be negligible in this study.

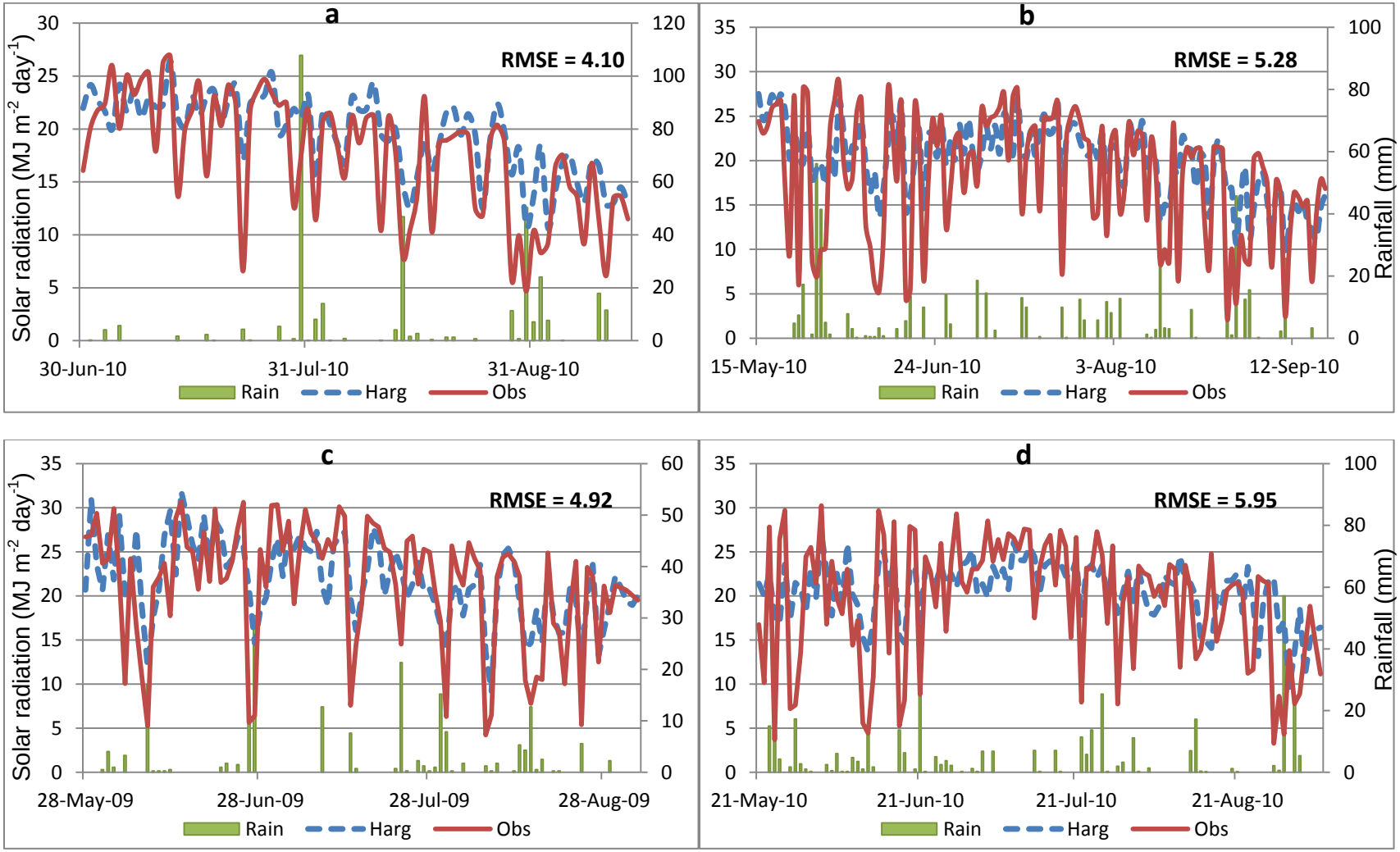
a
RMSE = 4.10
Solar radiation (MJ m-2 day-1)
30-Jun-10
31-Jul-10
31-Aug-10
Rain
Harg
Obs
b
RMSE = 5.28
Rainfall (mm)
15-May-10
24-Jun-10
3-Aug-10
12-Sep-10
Rain
Harg
Obs
c
RMSE = 4.92
Solar radiation (MJ m-2 day-1)
28-May-09
28-Jun-09
28-Jul-09
28-Aug-09
Rain
Harg
Obs
d
RMSE = 5.95
Rainfall (mm)
21-May-10
21-Jun-10
21-Jul-10
21-Aug-10
Rain
Harg
Obs

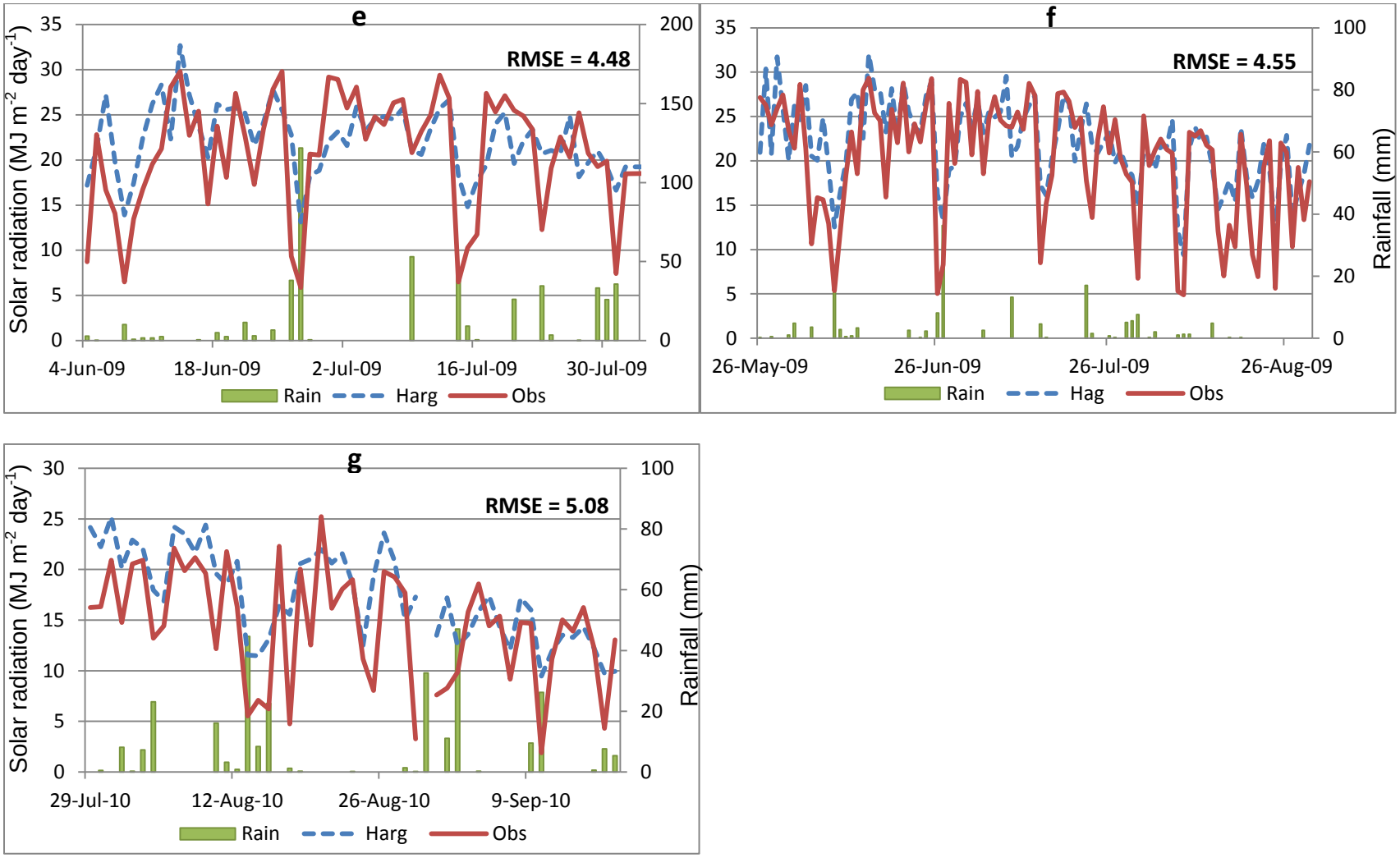

Fig 3.1 Comparison of Observed Incoming Solar Radiation and the Hargreaves Equation at (a) Elm Creek 2010, (b) Kelburn 2010, (c) Oakville 2009, (d) Morden 2010, (e) Kelburn 2009, (f) Portage 2009 and (g) Warren 2010.

3.4.2 FAO-56 ET_o versus the Priestley-Taylor Model

Daily ET_0 results from the Penman-Monteith (FAO 56 - equation 3.10) were compared to results obtained from the Priestley-Taylor (PT - equation 3.6) using observed incoming solar radiation as input. The analyses showed that the PT equation underestimated ET_o at all the sites considered (Table 3.3, Fig 3.2). A total of 644 days covering the growing season at seven site-years gave an overall RMSE value of 0.88mm day^{-1} with a mean bias error of -0.42. The percentage mean deviation from measured value was -14.2% (Table 3.3). A paired t-test showed that the difference observed between FAO-56 derived ET_o and the PT derived ET_o was statistically significant at 0.05 α level (Table 3.4).

Table 3.3 FAO-56 Daily ET_o versus the PT Model.

Site	*n*	*RMSE*	*MBE*	*%MD*
Elm Creek 2010	76	0.66	-0.50	-16.2
Kelburn 2009	85	0.89	-0.41	-13.7
Kelburn 2010	128	1.01	-0.57	-18.0
Morden 2010	109	0.89	-0.43	-14.6
Oakville 2009	99	0.75	-0.01	-2.9
Portage 2009	97	0.91	-0.43	-12.2
Warren 2010	50	0.97	-0.74	-27.3
Total	**644**	**0.88**	**-0.42**	**-14.2**

Table 3.4 Paired Two Sample t-test (PT vs FAO-56).

	Priestley-Taylor	*FAO-56*
Mean	3.48	3.90
Standard Deviation	1.53	1.38
Observations	644	644
Pearson Correlation	0.86	
Hypothesized Mean Difference	0	
Df	643	
t Stat	-13.9	
P(T<=t) one-tail	6.1E-39	
t Critical one-tail	1.65	
P(T<=t) two-tail	1.2E-38	
t Critical two-tail	1.96	
α	0.05	

This result agrees with the finding of Kashyap and Panda (2001) that the Priestley-Taylor equation underestimates ET_o though the magnitude of underestimation obtained in this result is higher than that of Kashyap and Panda (Table 3.1). Figure 3.2 shows the daily FAO 56 ET_o versus PT for the seven sites that had measured incoming solar radiation. Fig 3.2h shows that a significant part of the underestimation occurs when the FAO-56 daily ET_o values exceed 6mm. The study conducted by Kashyap and Panda (2001) showed that PT underestimated daily ET_o at observed values greater than 5mm.

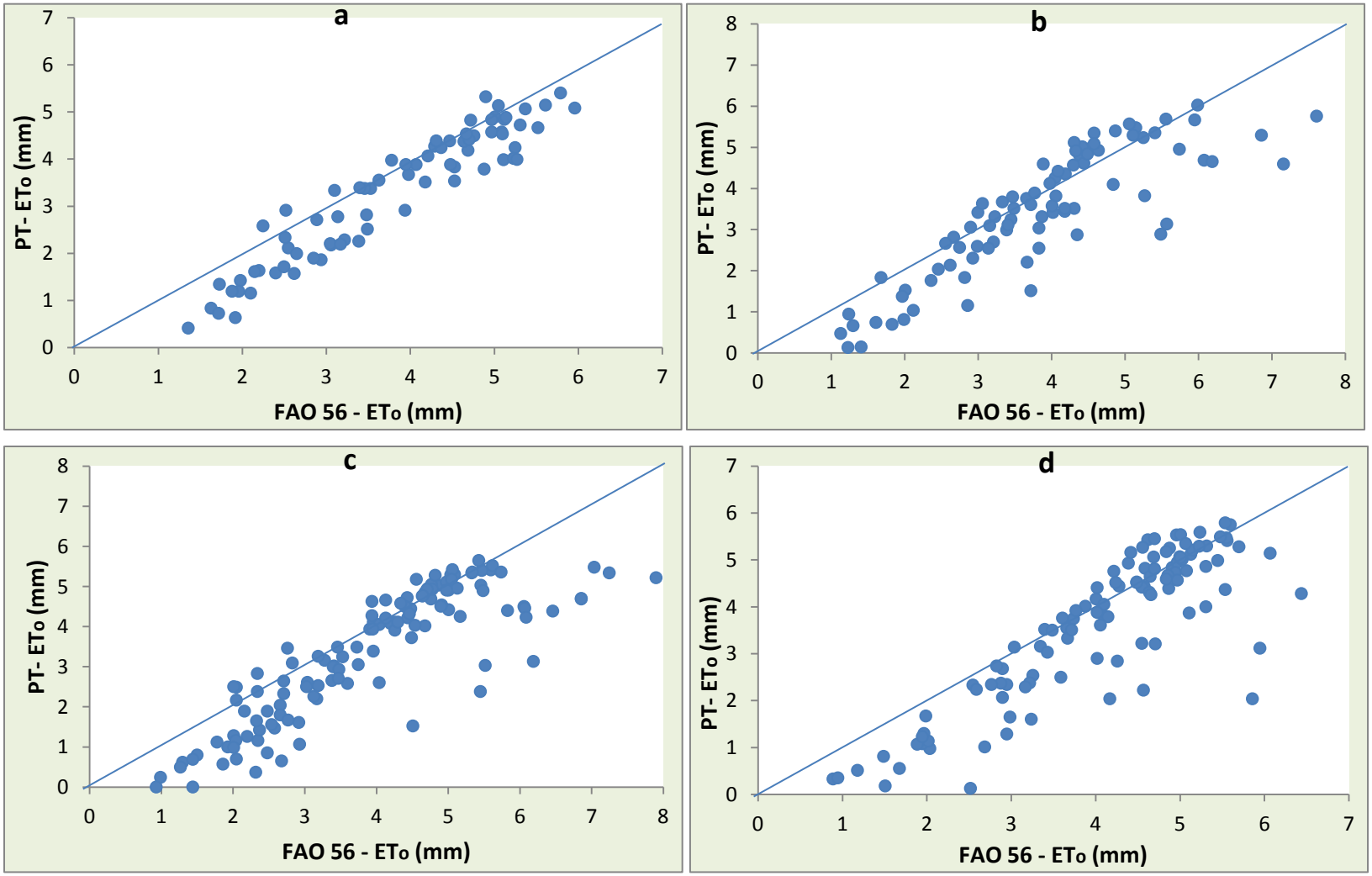
a
PT- ETo (mm)
FAO 56 - ETo (mm)
b
PT- ETo (mm)
FAO 56 - ETo (mm)
c
PT- ETo (mm)
FAO 56 - ETo (mm)
d
PT- ETo (mm)
FAO 56 - ETo (mm)

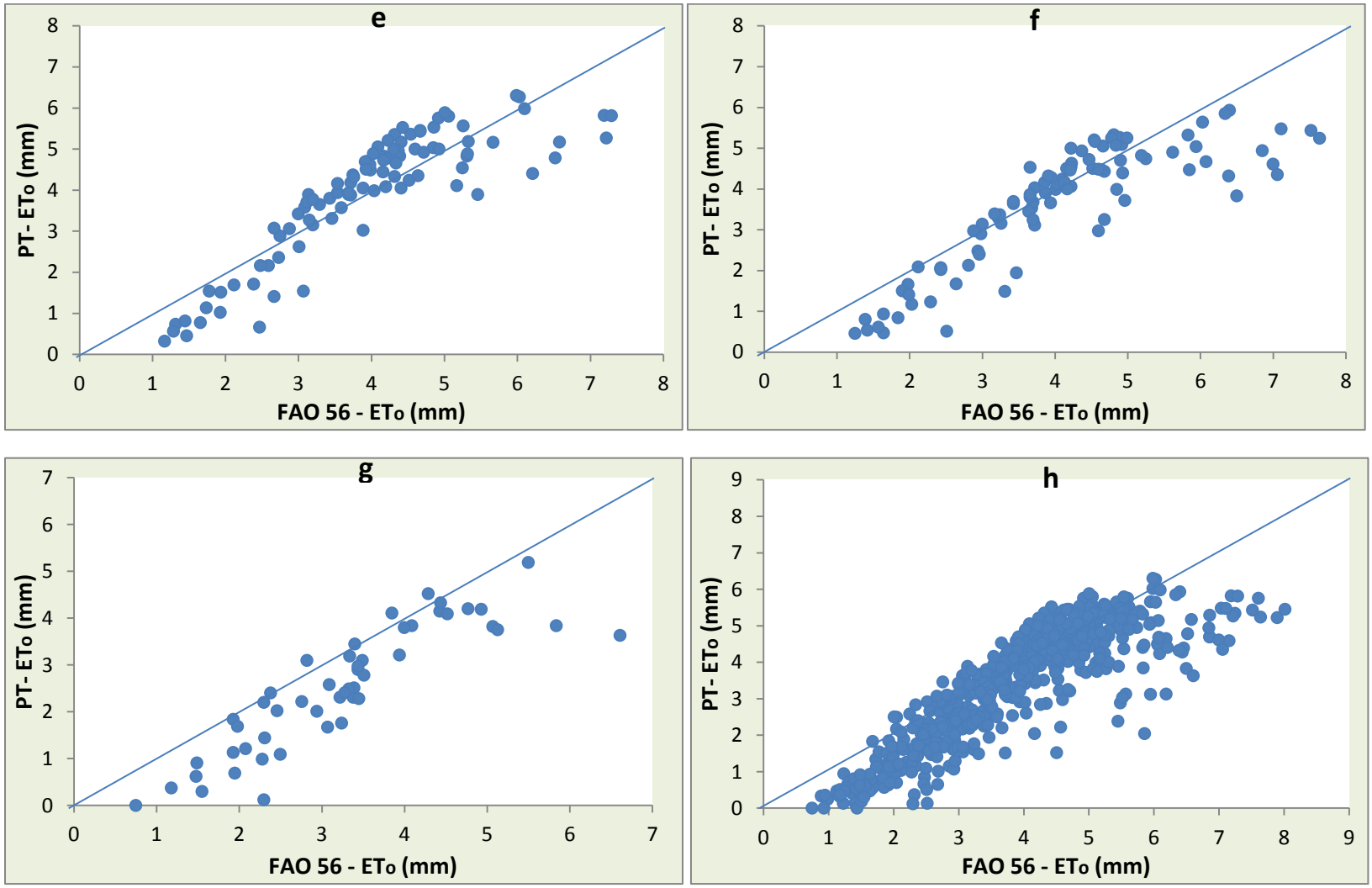

Fig 3.2 Daily FAO 56 ET_o versus PT for (a) Elm Creek 2010; (b) Kelburn 2009; (c) Kelburn 2010; (d) Morden 2010; (e) Oakville 2009; (f) Portage 2009; (g) Warren 2010 and (h) All sites combined.

3.5 Conclusion

Operational models, such as the VSMB, with a wide range of applications should be subjected to periodic modification based on evolving technology and current research findings to improve their output performance. The replacement of solar radiation data using Hargreaves' equation with observed, sensor-determined values is an improvement in accurately determining reference evapotranspiration. The inability of the Hargreaves' equation to effectively predict solar radiation especially at low extremes is an issue for calculating accurate evapotranspiration on those days. Likewise, the comparison between the Penman-Monteith and the Priestley-Taylor ET_o revealed an underestimation on days with high ET_o which is an issue for those days. Furthermore, these problems can have a cascading effect on model accuracy since they influence daily soil moisture values which are in turn influenced by estimates from previous days.

Underestimation of ET_o by the PT equation reduces the amount of water loss to the atmosphere and this directly impacts the accuracy of soil moisture estimates. The replacement of the PT ET_o with the FAO-56 is expected to slightly increase the drying rate of the soil layers and improve the accuracy of soil moisture estimation.

3.6 References

Akinremi, O.O. and McGinn, S. M. 1996. Usage of soil moisture models in agronomic research. Can. J. Soil Sci. **76:** 285–295.

Allen, R.G., Pereira, L.S., Raes, D. and Smith, M. 1998. Crop Evapotranspiration: Guidelines for Computing Crop Water Requirements, FAO Irrigation and Drainage Paper No 56, FAO, Rome.

Baier, W. and Robertson, G.W. 1966. A new versatile soil moisture budget. Can. J. Plant Sci. **46:** 299–315.

Bugbee, B. and Tanner, B. 2001. Long-term stability of five types of pyranometers in continuous field use. Presentation at ASA 2001. [Available] Online: http://www.usu.edu/cpl/Bruce%20revised%20pyranometer%20talk%20ASA%202001.pdf [2011,September 11].

De Jong, R. 1981. Soil water models: A review. LRRI Contribution No. 123. Agriculture Canada, Research Branch, Ottawa, ON.

Doorenbos, J. and Pruitt, W.O. 1977. Guidelines for predicting crop water requirements. Revised 1997. FAO Irrigation Drainage Paper No. 24. FAO Rome, Italy, 193 pp.

FAO.1986. Irrigation Water Management: Irrigation water needs. Training Manual No 3. [Online] Available: http://www.fao.org/docrep/S2022E/s2022e07.htm#TopOfPage [2011 April 4].

Hargreaves, G.H. and Samani, Z.A. 1985. Reference crop evapotranspiration from temperature. Applied Engineering Agriculture **1:** 96–99.

Howell, T.A. and Evett, S.R. 2004. The Penman-Monteith Method. Section 3 in Evapotranspiration: Determination of Consumptive Use in Water Rights Proceedings. Continuing Legal Education in Colorado, Inc. Denver, CO.

Jensen M.E. (ed.). 1973. Consumptive use of water and irrigation water requirements. American Society of Civil Engineering, New York, 215 pp.

Kashyap, P.S. and Panda, R.K. 2001. Evaluation of evapotranspiration estimation methods and development of crop-coefficients for potato crop in a sub-humid region. Agricultural Water Management. **50:** 9-25.

Lopez-Urrea, R., Martin de Santa Olalla, F., Fabeiro, C. and Moratalla, A. 2006. Testing evapotranspiration equations using lysimeter observations in a semiarid climate. Agricultural Water Management **85:** 15–26.

Monteith, J.L. 2000. Agricultural Meteorology: evolution and application. Agricultural and Forest Meteorology, **103:** 5-9.

Penman, H.L. 1948. Natural Evaporation from Open Water, Bare Soil and Grass. Proceedings of the Royal. Society of London. **193:** 120-145.

Pereira, A.R., Sentelhas, P.C., Folegatti, M.V., Villa Nova, N.A., Maggiotto, S.R. and Pereira, F.A.C. 2002. Substantiation of the daily FAO-56 reference evapotranspiration with data from automatic and conventional weather stations. Revista Brasileira de Agrometeorologia. **10:** 251–257.

Priestley, C.H.B. and Taylor, R.J. 1972. On the assessment of surface heat-flux and evaporation using large-scale parameters. Monthly Weather Review **100:** 81–92.

Sentelhas, P.C., Gillespie, T.J. and Santos, A.E. 2010. Evaluation of FAO Penman–Monteith and alternative methods for estimating reference evapotranspiration with missing data in Southern Ontario, Canada. Agricultural Water Management **97:** 635–644.

Shepherd, A. and McGinn, S.M. 2003. Assessment of climate change on the Canadian prairies from down-scaled GCM data, Atmosphere-Ocean. **41:**301-316.

Stannard, D.I. 1993. Comparison of Penman–Monteith. Shuttleworth–Wallace, and modified Priestley–Taylor evapotranspiration models for wildland vegetation in semiarid rangeland. Water Resources Management. **29:** 1379–1392.

Suleiman, A.A. and Hoogenboom, G. 2007. Comparison of Priestley–Taylor and FAO-56 Penman–Monteith for daily reference evapotranspiration estimation in Georgia, USA. Journal of Irrigation and Drainage Engineering. **133:** 175–182.

Thornthwaite, C.W. 1948. An approach toward a rational classification of climate. Geographical Review. **38:** 55–94.

Xing, Z., Chow, L., Meng, F.R., Rees, H.W., Stevens, L. and Monteith, J. 2008. Validating evapotranspiration equations using Bowen Ratio in New Brunswick. Maritime Canada. Sensors. **8:** 412–428.

4. VSMB Model Modification and Validation

4.1 Abstract

Changes were made to the Versatile Soil Moisture Budget which involved the improvement of ET_o estimates using direct solar radiation data and the Penman Monteith FAO-56 equation. These changes were expected to improve the model's performance in estimating soil moisture. Soil moisture outputs from the modified model (VB_1) were compared to the original model (VB_0) and the field-calibrated hydra probe values to validate the improvement in model performance. Results obtained showed that changes to ET_o in VB_1 did not significantly improve soil moisture estimates in 9 of the 13 field-years. The soil moisture RMSE for both VB_1 to VB_0 for all the sites was between 0.003 m^3 m^{-3} and 0.011 m^3 m^{-3}. A comparison of depth specific observed soil moisture values (Obs) to modelled values (VB_1) showed that the model was able to capture the trend in soil moisture changes effectively especially at the rapidly changing shallow depths of 5 cm and 20 cm. The RMSE of the comparison between the modelled and observed soil moisture at 5 cm depth for the fields was between 0.033 m^3 m^{-3} and 0.125 m^3 m^{-3}. However, at 100 cm depth, the RMSE was between 0.103 m^3 m^{-3} and 0.244 m^3 m^{-3}. A common trend of increasing RMSE at increasing depth was observed at most of the field-years. The total soil profile comparison showed that the model largely underestimated soil moisture at all site-years with very high RMSE, up to 192 mm at the Gladstone site. This was due to the model's assumption that the soil was drying out based on crop demand when in reality; the soil remained very wet due to a shallow water table.

4.2 Introduction

Models are used to predict the outcome of phenomena or to simply fill the gap between the ‘explainable or known’ and the ‘unexplainable or unknown’. Over the past four decades, the use of models have gained wide acceptance among researchers and this has resulted in the steady increase in the number of papers published using models (Monteith, 2000). Models have been vital in the advancement of science and continue to be an important tool. In the case of soil moisture estimation, models are cheaper and less laborious when compared to the cost of instrumentation for direct measurement, the amount of work required for installation and the level of expertise involved. However, models require validation using observed data to ensure that modelled results are accurate reflections of the real world.

Soil moisture sensors are often useful for point measurements and this poses a challenge in making general conclusions about the moisture content of an entire field, especially in fields with high spatial soil variability. Thus, several models have been developed to estimate soil moisture content. Some of these models include LEACHM, SHAW and VSMB. Leaching Estimation and Chemistry Model (LEACHM) is a process-based model developed by Hutson and Wagnet in 1984 to describe water and solute transport in unsaturated soils in one dimension. It has been used to simulate water and other dissolved solute transport through layered and non-homogenous soil profiles but a major drawback is that it cannot simulate soils with layers of unequal depth (Dodds et al., 1998).

Simultaneous Heat and Water (SHAW) model was originally developed to simulate soil freezing and thawing, heat, water and solute transfer within a one-dimensional profile (Flerchinger and Saxton, 1989; Flerchinger 2000). Both the heat and water fluxes are solved simultaneously and thus, the model requires initial soil temperature, a variable that is not widely available.

The VSMB was developed to simulate vertical, one-dimensional soil moisture fluxes. It has been widely used and validated under several conditions with modifications (Dyer and Mack 1984; Baier 1990; Hayhoe et al 1993; Baier and Robertson 1996; Akinremi et al 1996; Hayashi et al 2010). The VSMB model was selected for this study because of its capability to utilize user-defined depth for soil layer thickness, readily available inputs as well as its wide use and application in the Canadian prairies.

The performance of a model depends on the accuracy of its inputs. Substituting solar radiation input data estimated from the Hargreaves equation with observed input data as well as replacing the Priestley-Taylor ET_o equation with the Penman Monteith FAO-56, which has been widely reported to give better ET_o estimates (Kashyap and Panda, 2001; Pereira et al., 2002; Lopez-Urrea et al., 2006; Suleiman and Hoogenboom, 2007; Xing et al., 2008), was expected to improve the overall accuracy of soil moisture estimation by the VSMB. The objective of this study was to verify that the modifications made to the VSMB resulted in improvement in its ability to simulate soil water content.

4.3 Methods

4.3.1 The VSMB Model Overview

The Versatile Soil Moisture Budget (VSMB) was developed to simulate vertical, one-dimensional soil moisture flux. For close to five decades since its first introduction by Baier and Robertson (1966), it has undergone various modifications. The computer program was first described by Baier et al. (1972) and subsequently improved (Baier et al. 1979). Dyer and Mack (1984) described the VSMB Version 3, with further improvements, incorporating a drainage algorithm and a field performance appraisal. Boisvert et al. (1992) developed version 4 of the VSMB including a water-table function (Baier and Robertson 1996). Akinremi et al (1996) replaced the Baier-Robertson equation which uses temperature and latitude to estimate reference evapotranspiration with the Priestley-Taylor equation which uses solar radiation. They also incorporated a simple cascade algorithm adapted from the Ceres-Wheat model for infiltration and moisture redistribution. Hayashi et al (2010) modified the growth stage parameters and the drying curve function for grasslands. Estimates from the VSMB have been verified against lysimeter readings, soil moisture measurements and results from other techniques under a variety of climates, soil and crop conditions (Dyer and Mack 1984; Baier 1990; Hayhoe et al 1993; Baier and Robertson 1996; Akinremi and McGinn 1996; Hayashi et al 2010). In these comparisons, the VSMB gave reasonable estimates of soil moisture distribution. Based on the various modifications to the model by many scientists, different

versions of the model exist but the model used in this research was from Akinremi et al (1996).

The VSMB has been widely applied in agrometeorology and hydrology applications such as estimation of evaporation from grassland (Hayashi et al 2010), impact of water use on crop yields (Qian et al, 2009), number of field work days for manure application (Sheppard et al 2007), impact of climate change scenarios on the agro-climate of the Canadian prairies (McGinn and Sheppard, 2003), as well as the estimation of annual nitrous oxide emission (Corre et al 1999).

The VSMB works on a daily time-step with the soil column divided into a user-defined number of layers up to a maximum of six. The model uses two input files: a weather data file and soil/plant information file. These files are arranged in formats specified in the VSMB source code. Three volumetric soil moisture parameters are required (expressed in mm):

Field capacity (θ_{FC}), which is the amount of water the soil can hold after downward movement due to gravity has stopped.

Saturation (θ_{SAT}), which is the total amount of water in the soil after all the pore spaces have been filled.

Permanent Wilting Point (θ_{PWP}), which is the lowest boundary of plant available soil moisture below which plants can no longer extract water.

Soil moisture held at field capacity was determined *in-situ* using the procedure outlined in Appendix A. Soil samples were subjected to a pressure of

1.5 MPa to determine the water content at permanent wilting point. Saturation water content is equivalent to soil total porosity which was derived from bulk density as shown in Equation 4.1.

$$\theta_{SAT} = Porosity = \left(1 - \frac{P_B}{P_D}\right) \quad (4.1)$$

where P_B is the bulk density and P_D is the particle density which was assumed to be 2.65g cm^{-3}. The three soil moisture parameters are input as mm of water for each soil layer. The volumetric saturation water content can be converted to mm of water using:

$$SAT\ (mm) = \Delta z_i(\theta_{SAT})\ 10^3 \quad (4.2)$$

where Δz_i is the thickness of the soil layer in meters.

The initial water content of the soil is needed for the first day of the time period being simulated. The soil moisture content changes thereafter based on precipitation gain, evapotranspiration loss, infiltration and drainage. The soil water content in a layer (*i*) is given by:

$$W_i = \Delta z_i(\theta_i)\ 10^3 \quad (4.3)$$

The model drains excess water above field capacity from the *i*-th layer (*i* = 1 at the topmost layer) to the one below it (*i*+1 layer) in one day and no further drainage occurs until the water content exceeds field capacity again. This poses a limitation to the model since some soils, especially, heavy soils, hold water

above field capacity for more than a day. The available water holding capacity (W_{Ci}, mm) of the *i*-th soil layer is defined by:

$$W_{Ci} = \Delta z_i(\theta_{FC} - \theta_{PWP})\, 10^3 \qquad (4.4)$$

In addition to the gravitational drainage of soil layers described above, Akinremi *et al.* (1996) adopted the Ceres algorithm from Ritchie and Otter (1985) for diffusive exchange of soil water between the *i*-th and *i*+1-th layer. Hayashi *et al.* (2010) presented the equation as:

$$q_i = -10^3 D_h(\theta_A)\, \frac{\partial \theta_A}{\partial z} = -10^3 D_h \left(\frac{\theta_{Ai} + \theta_{Ai+1}}{2}\right) \frac{\theta_{Ai+1} - \theta_{Ai}}{z_{i+1} - z_i} \qquad (4.5)$$

where D_h ($m^2\ d^{-1}$) is hydraulic diffusivity, θ_{Ai} (= $\theta_i - \theta_{PWPi}$) is the available water content of the *i*-th layer, and z_i (m) is the depth to the center of the *i*-th layer. Since z increases downward, a positive value of q_i indicates downward flow. The D_h function is defined by:

$$D_h = min[0.88 \exp(35.4\theta_A), 100] \qquad (4.6)$$

where min[,] indicates the minimum of the two values.

The VSMB has the capability of running year-round with effective snow-budget simulations. However, the scope of this research is limited to the growing season. Several subroutines, which are programs within a main program required to perform specific operations and return the result as an input in the main program, are used in VSMB. Some of the subroutines include a plant growth simulation subroutine and a reference evapotranspiration subroutine. The main

output from the model is the simulated volumetric soil water content at the various depths specified by the user. Other outputs, which also serves as inputs include, the top of the atmosphere radiation, maximum sunshine hours, reference and actual evaporation.

The versatile soil moisture budget outputs daily volumetric soil moisture based on user-defined soil depths using a moisture balance approach. Soil moisture balance at the surface layer is given as:

$$\theta v_{ij} = \theta v_{i-1,j} + P_i - RO_i - ET_{ij} - D_{ij} \quad (4.7)$$

θv_{ij} is the water retained on day i at soil depth j, $\theta v_{i-1,j}$ is the water content from the previous day at depth j, $P_i - RO_i$ is the precipitation less runoff for the surface layer (or simply I_{ij} which is infiltration into layer j on day i), ET_{ij} is the evapotranspiration loss and D_{ij} is drainage loss to the adjacent layer.

For the purpose of this study, the depths modelled correspond with the depths monitored with the hydra probes. However, since the model cannot handle gaps in the soil moisture profile, the gaps were filled as shown in Table 4.1. Four hydra probes were installed at 5 cm, 20 cm, 50 cm and 100 cm respectively but the VSMB soil moisture outputs were simulated at five depths since all the necessary input parameters to run the model for the extra depth (at 35 cm) were available.

Table 4.1 Probe Installation and Sampling Depths

Soil Sampling Range (cm)	Installed Hydra Probe (cm)	VSMB Simulation Range (cm)	VSMB Central Points (cm)
0-10	5	0 - 12.5	5
15-25	20	12.5 - 27.5	20
30-40*****	-	27.5 - 42.5	35
45-55	50	42.5 - 57.5	50
95-105	100	57.5 - 105.5	100

***** No measured soil moisture at this depth, though simulated by the model.

The Soil Conservation Service (SCS) runoff curve number (USDA-NRCS 2004, Table 9-1) used in the original VSMB was retained to determine rainfall surface runoff. However, field-specific values were used based on the soil texture of the topmost layer as well as the type of crop planted (Table 4.2). Root extraction coefficients used by Akinremi et al. (1996), obtained from Baier et al. (1979), were retained but adjusted for difference in soil depth (Table 4.3).

Table 4.2 SCS Runoff Curve Number Table

	< 10% Clay, > 90% Sand	10-20% Clay, 50-90% Sand	20-40% Clay, < 50% Sand	40% Clay, < 50% Sand
Small Grains	63	76	84	88
Grass	68	79	86	89
Row Crops	67	78	85	89

Table 4.3 Root Extraction Coefficients (dimensionless)

Akinremi *et al.* (1996)	Depth (cm)				
	0 – 15	15 – 30	30 – 60	60 – 90	90 – 120
P – E	0.40	0.10	0.05	0.01	0.01
E – J	0.40	0.15	0.10	0.02	0.01
J – H	0.55	0.20	0.20	0.10	0.05
H – SD	0.55	0.25	0.25	0.15	0.05
SD – R	0.55	0.25	0.25	0.15	0.05

Modified Depth Diff	Depth (cm)				
	0 – 12.5	12.5 – 27.5	27.5 – 42.5	42.5 – 57.5	57.5 - 105.5
P – E	0.40	0.10	0.03	0.02	0.02
E – J	0.40	0.14	0.06	0.04	0.03
J – H	0.55	0.20	0.12	0.08	0.15
H – SD	0.55	0.25	0.15	0.10	0.20
SD – R	0.55	0.25	0.15	0.10	0.20

P = Planting, E = Emergence, J = Jointing, H = Heading, SD = Soft Dough, R = Ripening

The VSMB computes AET from individual soil layers using empirical factors dependent on soil moisture and plant condition:

$$AET = \sum_{i=1}^{n} [ET_o \times R_i \times DC(W_i/W_{ci})] \qquad (4.8)$$

where ET_o is the reference evaporation (from Penman Monteith FAO-56), R_i is the root coefficient (Table 4.3), DC is the drying curve and W_i/W_{ci} is the relative soil moisture content.

The drying curve (DC) function given in the VSMB is calculated as:

$$DC(x) = (x/C_r)^{C_m C_n C_h}((x/C_r)^{C_m}(C_n/x) + (C_m/C_r)((C_r - x)/C_r)^{C_n}) \qquad (4.9)$$

where x is the relative soil moisture content which is the ratio of soil water content to the water holding capacity of the soil, $C_m, C_n, C_h \; and \; C_r$ are dimensionless fitting parameters given as 1,1,1 and 0.7 respectively for cropped field and 1,1,1 and 0.5 respectively for fallow fields. The drying curve function dictates the relative ease of soil water loss from field capacity to permanent wilting point. This drying curve function represents curves E and D adapted by Akinremi et al (1996) from Baier et al (1979) for cropped and fallow soils respectively. Curve E assumes no reduction in AE:ET_o ratio over the range of available soil moisture from 100 – 50% and from 100 - 70% for curve D. Beyond these points, the AE decreases sharply with decreasing available soil moisture content.

Model sensitivity analysis carried out by Hayashi (2010) showed that the drying curve function (DC) and root coefficient (R_i) have a strong effect on the rate of actual evapotranspiration from each soil layer which in turn, influences the soil moisture content.

4.3.2 VSMB Model Modifications

The Akinremi et al. (1996) version of VSMB utilizes the minimum and maximum daily temperature, and precipitation. However, to accommodate the changes made, additional weather data were added to the VSMB weather input

file. Table 4.4 summarizes these modifications. Soil moisture output from the Akinremi et al. (1996) version of the model is hereafter referred to as VB_0 and results using the modified inputs are referred to as VB_1.

Table 4.4 Summary of modifications to Akinremi et al (1996) VSMB Version.

Parameter	Akinremi et al (1996)	Modified Version
Weather Input	Rainfall, maximum and minimum temperature	Rainfall, maximum and minimum temperature, maximum and minimum humidity, wind speed and solar radiation
Solar radiation (R_s)	Hargreaves	Data input from Pyranometer*****
Net radiation (R_n)	$R_n = 0.63R_s - 40$	$R_n = R_{ns} - R_{nl}$
ET_o	Priestley-Taylor	Penman Monteith (FAO-56)*****
Vegetation	Wheat	Wheat, Canola (P-day) and Grass (heat accumulation)

***** Used if data is available, otherwise, Akinremi et al (1996) is used
R_{ns} net incoming shortwave radiation [MJ m^{-2} day^{-1}]
R_{nl} net outgoing longwave radiation [MJ m^{-2} day^{-1}]

4.3.3 Plant Growth Simulations

Evapotranspiration from a bare field is largely due to evaporation from the soil surface. However, as vegetation grows and shades the soil surface from direct sunlight, ET gradually shifts to being largely dependent on transpiration. Plant type, height, density, growth stages, root depth, canopy resistance and other crop characteristics play an important role in water loss from vegetative

surfaces. Plant growth simulation is vital to accurate prediction of soil moisture fluxes.

Based on the need to simulate soil moisture content under different crop types, the VSMB input file was modified to include crop selection capability. The value of 1 is assigned to wheat crop, 2 for canola and 3 for grass growth simulation.

Growth Simulation of Wheat

VB_0 has an algorithm that simulates wheat and barley growth using the bio-meteorological time scale (Robertson, 1968). The coefficients of this growth simulation were developed from many fields in nine test sites across Canada and the algorithm developed calculates the daily rate of crop development using non-linear functions that depends on both daily temperature (maximum and minimum) and photoperiod. Five stages were specified for crop development from planting, usually denoted by the corresponding numbers:

Planting ⇨ Emergence ⇨ Jointing ⇨ Heading ⇨ Soft Dough ⇨ Maturity
(0) (1) (2) (3) (4) (5)

The subroutine called SMBTS performs this growth simulation in the VSMB model. However, if the actual phenology is known and included in the input file, the model uses this instead.

Shaykewich (1995) reviewed the responses of phenological development of some cereals (corn, wheat and barley) and concluded that the growth response to temperature of most species is sigmoidal, rather than linear. More recently, Saiyed et al. (2009) observed crop phenological stages and detailed weather data across 17 site-years in western Canada for six hard spring wheat varieties and tested the accuracy of bio-meteorological time (BMT), growing degree days (GDD), and physiological days (Pdays) for prediction of wheat phenological stages. They recommended the use of the BMT scale for estimation of wheat phenological development. This justifies the retention and use of BMT in the VSMB model if actual crop phenology is unknown.

Canola P-day

The Canola Council of Canada reported that the growth and development of a canola plant as well as the length of each growth stage is influenced by temperature, moisture, photoperiod, nutrition and variety. Of the environment-related factors, temperature is singled out as the most important factor regulating the growth and development of canola in western Canada.

Physiological days (P-days) is a temperature-based, crop growth simulation function originally developed for potatoes (Sands et al. 1979) but modified and used for canola growth (Shaykewich, 2001). Canola base, optimum and maximum temperatures were estimated to be 5˚C, 17˚C and 30˚C respectively. Heat accumulation is based on temperature weighted averages but

no P-day heat unit is accumulated at temperatures below the base level of 5˚C or above the maximum of 30˚C. Shaykewich (2001) gave the P-day heat accumulation equation as:

$$P - Days_{(5,17,30)} = \frac{1}{24} * [(5 * P(T_1) + 8 * P(T_2) + (8 * P(T_3) + 3 * P(T_4)] \quad (4.10)$$

where:

$T_1 = T_{min}$ (Minimum Temperature)

$T_2 = \frac{(2 * T_{min}) + T_{max}}{3}$

$T_3 = \frac{(2 * T_{max}) + T_{min}}{3}$

$T_4 = T_{max}$ (Maximum Temperature)

$P = 0 \quad When\ T < 5$

$P = k * \left[1 - \left(\frac{(T-17)^2}{(17-5)^2}\right)\right] \quad When\ 5 \leq T \leq 17$

$P = k * \left[1 - \left(\frac{(T-17)^2}{(30-17)^2}\right)\right] \quad When\ 17 \leq T \leq 30$

$P = 0 \quad When\ T \geq 30$

$Where\ k\ is\ a\ scale\ factor\ set\ to\ a\ value\ of\ 10$

Several developmental stages have been proposed for canola growth, however, to make it consistent with the five growth stages used in the BMT scale, a five-stage canola growth pattern was adopted as defined by Shaykewich (2001) with specific heat accumulation thresholds for advancing from one stage to the other (Table 4.5).

Table 4.5 Canola P-Days

Growth Stage	Cumulative P-days
Planting – Rosette	0 – 139
Rosette – Budding	140 – 299
Budding – Flowering	299 – 419
Flowering – Ripening	419 – 529
Ripening – Maturity	529 – 836

Growth Simulation of Grass

Another major modification to the VSMB model is the grass growth simulation. The VSMB has been used extensively for croplands, especially wheat, but little has been done on grasslands. Hayashi et al. (2010) used a three-phase growth stage approach for grasslands which is:

Dormant (1) ⇨ Growing (2) ⇨ Full Cover (3)

The developmental phase changes in response to heat unit accumulation. The growth stage goes from dormant (stage 1) to growing (stage 2) when the daily mean temperature exceeds 1˚C for five consecutive days, and from growing (stage 2) to full cover (stage 3) when cumulative growing degree day (GDD) reaches 240. The growth stage goes back to dormant when the maximum sunshine duration is below 10.5 hour (Hayashi et al., 2010).

$$T_{GDD} = \frac{T_{max} + T_{min}}{2} - T_b \quad (4.11)$$

where T_{max} and T_{min} are daily maximum and minimum air temperatures (˚C) respectively, T_b is the base temperature which is set to 5˚C for grass.

4.3.4 Soil Moisture Content from Calibrated Hydra Probes

Detailed field and laboratory calibration were carried out on the FDR sensors to ensure that the data from these hydra probes truly reflect the soil moisture content. Field calibration equations were observed to have the lower RMSE than the laboratory derived equations and the factory default equation. Thus, the field calibration equations (Table 4.6) were selected as the basis for observed soil moisture content. The calibration equations were derived for three soil categories based on clay content.

Table 4.6 Field Calibration Equations

Category	Equation	R^2
A	0.09704x - 0.12478	0.83
B	0.07642x - 0.05692	0.57
CD	$-0.0007x^3 + 0.0725x^2 – 1.64x + 39.39$	0.56

where x is $\sqrt{\varepsilon_{TC}}$ (square root of temperature corrected real dielectric permittivity) in categories A and B, and ε (real dielectric permittivity) in category CD.

These equations, based on the soil's dielectric permittivity, comparatively reflect the observed soil moisture content. The FDR sensors provide hourly and daily dielectric permittivity values which can be used with the field-derived equations to give hourly or daily volumetric water content (m^3 m^{-3}). The soil moisture data from these hydra probes provide a basis for comparing the soil moisture output from the VSMB model.

4.3.5 Statistical Procedure

To evaluate the performance of the model to estimate soil moisture, the root mean square error (RMSE) was calculated as shown in Equation 4.12.

$$\mathrm{RMSE} = \left(\frac{\Sigma(modelled - measured)^2}{n}\right)^{0.5} \qquad (4.12)$$

where *modelled* is the soil moisture output from the VSMB model and *measured* is the result from soil moisture content using field-derived calibrations by texture category for the FDR sensors, and *n* is the number of observations.

The mean bias error (MBE) was calculated to determine overestimation or underestimation. Positive values of MBE indicated overestimation, while negative values indicated underestimation. If the MBE is 0, it means that there is equal distribution of positive and negative differences.

$$MBE = \frac{1}{n}\left[\sum_{i=1}^{N}(Modelled - Measured)\right] \qquad (4.13)$$

These statistics were also used to compare results between the original (VB_0) and modified (VB_1) VSMB. A two sample z-Test for means at alpha level of 0.05 was conducted in order to assess whether the results were significantly different from each other and from the measured values.

4.4 Results and Discussion

4.4.1 VB_1 versus VB_0 Soil Moisture

From the results obtained, changes to the model did not result in significant improvement in the soil moisture output of the model at most of the fields. Though the ET_o values derived from the FAO-56 PM were significantly different from ET_o values from Priestley-Taylor, the soil moisture content derived from both ET_o equations did not show any significant difference at alpha level of 0.05 except at the Treherne fields in both years (Table 4.7). This is reflected in the p-values of the z-test which were less than 0.05. Also, the RMSE for all the sites was between 0.003m^3 m^{-3} and 0.011m^3 m^{-3}. Expectedly, the MBE showed that the VB_1 estimates were lower than the VB_0 at 11 of the 13 site-years due to greater ET_o in the VB_1 from the FAO-56 model which dries the soil more than the PT model used in VB_0.

The change in ET_o did not result in a significant change in soil moisture at most fields and this might be as a result of the wet growing seasons under which the research was conducted. Larger differences may have been observed in drier or windy conditions. It was surprising to observe that the Treherne fields showed a significant difference between VB_1 and VB_0 at both fields for both years considered. Specific depth analysis showed that there was a significant difference between VB_1 and VB_0 only at 50 cm depth of Treherne Grass 2010 field (*n = 164*). There was no significant difference at the other depths. The

influence of a large sample number (*n*) likely played a role because very small differences can become significant as *n* becomes larger.

Table 4.7 Comparison between VB_1 and VB_0.

SITE	n*	Mean VB_1 ($m^3\ m^{-3}$)	Mean VB_0 ($m^3\ m^{-3}$)	RMSE ($m^3\ m^{-3}$)	MBE	p-value
Oakville Canola 2009	396	0.295	0.294	0.003	0.001	0.869
Portage Canola 2009	388	0.274	0.275	0.004	-0.001	0.706
Gladstone Grass 2009	612	0.170	0.173	0.004	-0.003	0.504
Kelburn Oat 2009	476	0.398	0.398	0.003	-0.001	0.806
Treherne Wheat 2009	576	0.194	0.199	0.007	-0.005	0.018**
Treherne Grass 2009	576	0.167	0.173	0.007	-0.006	0.024**
Carman Alfalfa 2010	580	0.278	0.277	0.003	0.001	0.809
ElmCreek Canola 2010	500	0.216	0.221	0.006	-0.005	0.126
Morden Wheat 2010	436	0.309	0.312	0.004	-0.003	0.680
Kelburn Wheat 2010	512	0.370	0.372	0.005	-0.002	0.600
Treherne Canola 2010	656	0.183	0.187	0.007	-0.004	0.047**
Treherne Grass 2010	656	0.178	0.184	0.011	-0.006	0.007**
Warren Grass 2010	218	0.378	0.381	0.007	-0.003	0.485

* n is the combination of the daily output for all four depths
** p-value < 0.05 implies that mean difference is significant.

4.4.2 Depth Specific Field-Derived Calibration versus Modelled (VB_1) Soil Moisture

Analysis of the thirteen site-years (Fig 4.1A-C) showed that the model was able to capture the trend in changes to soil moisture especially at the 5 cm and 20 cm depths where soil moisture changes rapidly. The RMSE of the comparison

between the modelled and the soil moisture from field-derived calibration at 5 cm depth for the fields was between 0.033m^3 m^{-3} and 0.125m^3 m^{-3}. However, at 100 cm depth, the RMSE was between 0.103m^3 m^{-3} and 0.244m^3 m^{-3} (Table 4.8). There was a common trend of increasing RMSE as depth increases for most site-years. This may be due to the drying curve coefficients which dry the soil at lower depths faster than observed. The exclusion of water table depth as a factor in the model might have also played a significant role in the high RMSE observed at lower depths. The model assumes that soils dry out based on plant root demand and acquire moisture from the adjacent moist layer after a rainfall event. However, when some soil profiles were dug in the spring (e.g. at Elm Creek, Gladstone and Warren), the water table was very shallow (about 60 cm). This certainly influenced soil moisture content at 50cm and 100cm depths but is not taken into account by the VSMB.

The MBE at the surface layer (5 cm) showed that in nine of the thirteen site-years, the model overestimated soil moisture (Table 4.8). However, at all other depths (20 cm, 50 cm and 100 cm), all the site-years showed a consistent underestimation except at 20 cm depth at Kelburn Oat 2009. The consistent underestimation at depths reinforces the need to re-evaluate the drying curve. Oakville and Treherne canola fields had the lowest RMSE of 0.033m^3 m^{-3} at the surface depth and Warren grass field had the highest RMSE of 0.125m^3 m^{-3}. The Warren grass, heavy clay field exemplifies the problem in situations where the model simulates rapid drying of soil moisture from saturation to field capacity in a single day when in reality the soil remains above field capacity for days.

The results obtained were similar to Akinremi et al (1996) where the soil moisture content in the surface layer was simulated with greater accuracy than at the lower depths. However, unlike the findings in this research, the modifications made by Akinremi et al (1996) compared better with measured values than those simulated using the original VSMB version they worked with. The modification to the VSMB carried out in this study is unique because no other modification to this model has focused on changing the evapotranspiration subroutine, substituting the Priestley-Taylor ET_o with the Penman Monteith ET_o.

Table 4.8 Comparison of modelled versus field-derived calibration soil moisture

	RMSE(m^3 m^{-3})			
SITE/ DEPTH	**5**	**20**	**50**	**100**
Oakville Canola 2009	0.033 (0.009)	0.155 (-0.154)	0.148 (-14.2)	0.107 (-0.102)
Portage Canola 2009	0.082 (-0.061)	0.126 (-0.122)	0.107 (-10.4)	0.153 (-0.149)
Gladstone Grass 2009	0.093 (-0.091)	0.097 (-0.094)	0.186 (-18.2)	0.244 (-0.230)
Kelburn Oat 2009	0.105 (0.100)	0.044 (0.007)	0.049 (-3.9)	0.150 (-0.054)
Treherne Wheat 2009	0.044 (0.006)	0.080 (-0.071)	0.096 (-9.2)	0.123 (-0.122)
Treherne Grass 2009	0.038 (-0.004)	0.062 (-0.047)	0.087 (-7.6)	0.103 (-0.095)
Carman Alfalfa 2010	0.043 (0.010)	0.087 (-0.081)	0.176 (-17.3)	0.145 (-0.139)
ElmCreek Canola 2010	0.089 (0.063)	0.075 (-0.063)	0.160 (-15.9)	0.198 (-0.196)
Morden Wheat 2010	0.038 (0.025)	0.075 (-0.073)	0.076 (-7.1)	0.207 (-0.205)
Kelburn Wheat 2010	0.047 (0.027)	0.063 (-0.050)	0.125 (-12.0)	0.168 (-0.164)
Treherne Canola 2010	0.033 (0.015)	0.084 (-0.080)	0.147 (-14.4)	0.219 (-0.218)
Treherne Grass 2010	0.041 (0.023)	0.066 (-0.063)	0.085 (-0.080)	0.189 (-0.188)
Warren Grass 2010	0.125 (-0.104)	0.117 (-0.111)	-	-

Values in brackets are the MBE. Negative values show that the model underestimated observed soil moisture.

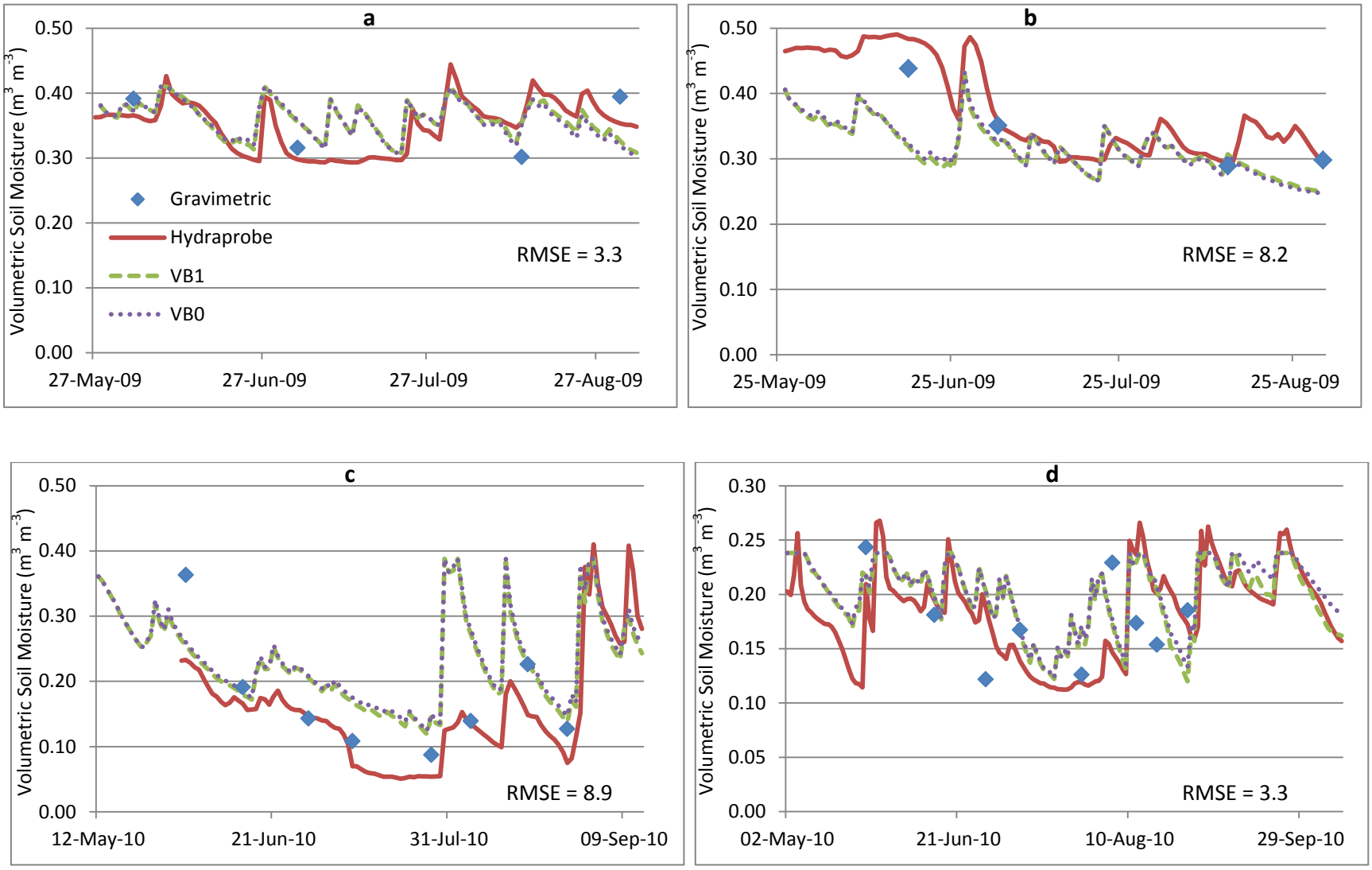

Fig 4.1A: Soil moisture time series at 5cm depth at (a) Oakville 2009; (b) Portage 2009; (c) Elm Creek 2010 and (d) Treherne Canola 2010.

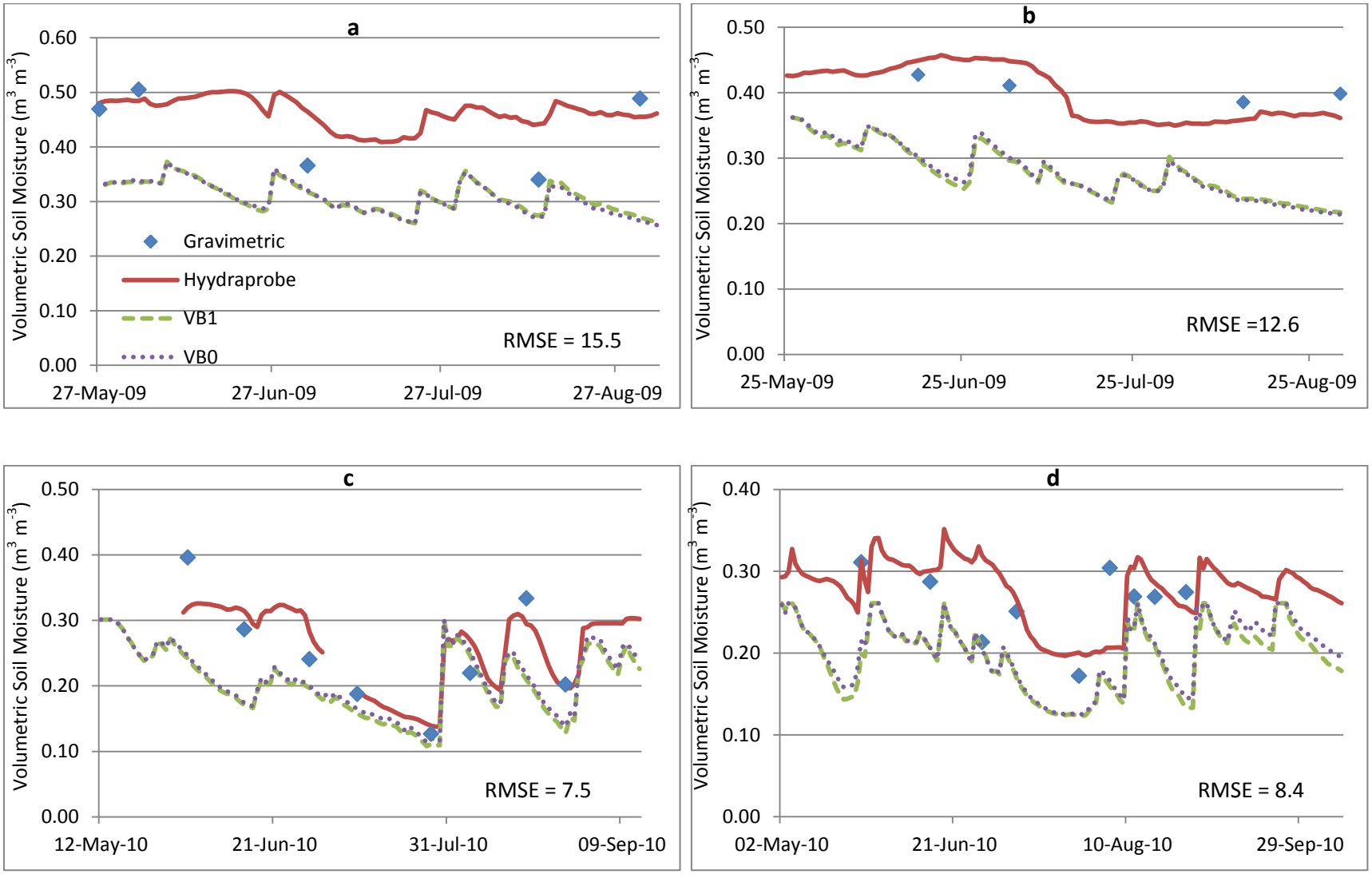

Fig 4.1B: Soil moisture time series at 20cm depth at (a) Oakville 2009; (b) Portage 2009; (c) Elm Creek 2010 and (d) Treherne Canola 2010.

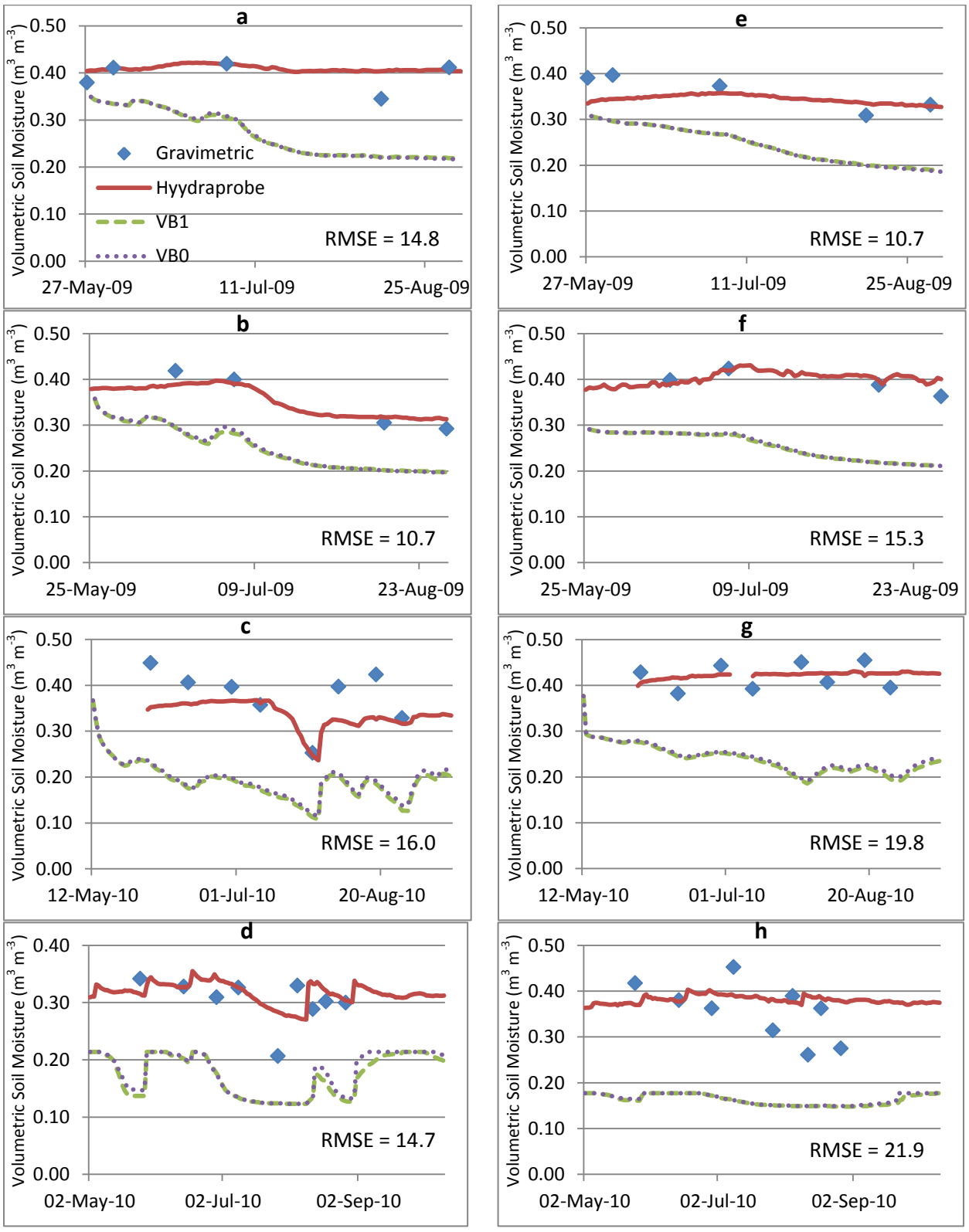

Fig 4.1C: Soil moisture time series at 50 cm (a-d) and 100 cm depths (e-h) at Oakville 2009, Portage 2009, Elm Creek 2010 and Treherne Canola 2010 fields respectively.

4.4.3 Profile comparison of modelled versus field-derived calibration soil moisture

The comparison of observed soil moisture contained in the soil profile (0-105 cm) to the modelled output showed that the VB_1 consistently underestimated soil moisture, as observed from the negative MBE for all site-years (Table 4.9). This was largely due to the underestimation observed at the lower depths. All the RMSE were very high with the highest observed at Gladstone Grass 2009 at 192.1mm. This was mainly as a result of the high water table which influenced the observed soil moisture. The model could not simulate the high water table and assumed that the soil was drying out based on crop demand.

Table 4.9 Profile comparison of modelled versus field-derived calibration soil moisture.

SITE	n	RMSE(mm)	MBE(mm)
Oakville Canola 2009	99	115.2	-111.5
Portage Canola 2009	97	128.6	-127.1
Gladstone Grass 2009	133	192.1	-184.7
Kelburn Oat 2009	76	54.3	-44.5
Treherne Wheat 2009	135	96.1	-94.5
Treherne Grass 2009	135	76.6	-74.9
Carman Alfalfa 2010	144	123.6	-119.6
ElmCreek Canola 2010	99	136.5	-135.8
Morden Wheat 2010	77	127.8	-126.5
Kelburn Wheat 2010	127	118.2	-116.0
Treherne Canola 2010	163	151.6	-150.9
Treherne Grass 2010	163	120.9	-120.1
Warren Grass 2010**	102	39.4	-37.8

** Based on 0-25cm depth

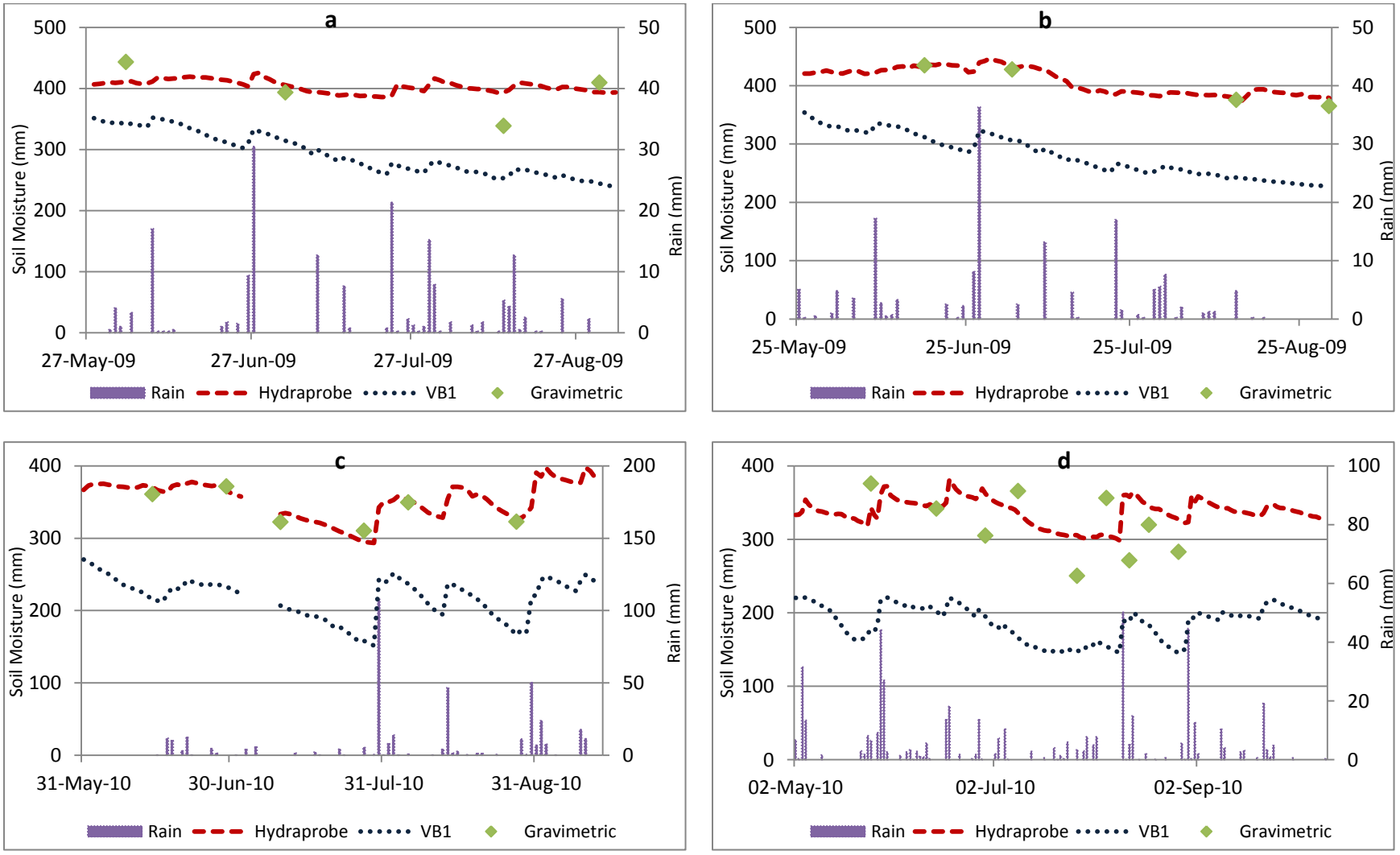

Fig 4.2 Rainfall, Observed and Modelled Soil Moisture at (a) Oakville 2009 (b) Portage 2009 (c) Elm Creek 2010 and (d) Treherne Canola 2010.

4.5 Conclusion

The use of models has many potential benefits. However, modelled results should be comparable to observed values before such models can be used in planning and decision making processes. The VSMB was modified by replacing the Priestley-Taylor ET_o equation with the Penman Monteith FAO-56 equation in a bid to improve its soil moisture estimation. This study showed that the modification to the original VSMB did not significantly improve its soil moisture estimation at most of the site-years. The model was most effective at simulating soil moisture content at the rapidly changing surface with a RMSE as low as 0.033 m^3 m^{-3} at some fields. At lower depths, however, the model greatly underestimated the observed values. At some locations, this was due to the model drying out soil moisture based on crop demand when in reality the water table was very shallow and was replenishing soil moisture at depth. The magnitude of soil moisture underestimation at such locations increased with increased data points such as at Gladstone 2009 which had the highest magnitude of underestimation with a value of -184.7 mm.

Further study that looks into the drying curve as well as the root extraction coefficients is recommended. Adding a subroutine to replenish soil moisture at depth for fields with a shallow water table would also be expected to improve the model's soil moisture prediction.

4.6 References

Akinremi, O.O. and McGinn, S. M. 1996. Usage of soil moisture models in agronomic research. Can. J. Soil Sci. **76:** 285–295.

Akinremi, O.O., McGinn, S.M. and Barr, A.G. 1996. Simulation of soil moisture and other components of the hydrological cycle using a water budget approach. Can. J. Soil Sci. **76:** 133–142

Baier, W. 1990. Characterization of the environment for sustainable agriculture in semi-arid tropics. R. P. Singh, ed. Sustainable agriculture. Issues, perspectives and prospects in semi-arid tropics. Proceedings of the International Symposium on Natural Resources Management for a Sustainable Agriculture, New Delhi, Indian Society of Agronomy. **1:** 90-128.

Baier, W., Chaput, D.Z., Russelo, D.A. and Sharp, W.R. 1972. Soil moisture estimator program system. Tech. Bull. No. 72. Agrometeorology Section, Plant Research Institute, Agriculture Canada, Ottawa. ON. 55 pp.

Baier, W. and Robertson, G.W. 1996. Soil moisture modelling - conception and evolution of the VSMB. Can. J. Soil Sci. **76:** 251-261.

Baier, W. and Robertson, G.W. 1966. A new versatile soil moisture budget. Can. J. Plant Sci. **46:** 299–315.

Baier, W., Dyer, J.A. and Sharp, W.R. 1979. The Versatiie Soil Moisture Budget. Tech. Bull. 87, Agrometeorology Section, Research Branch, Agriculture Canada, Ottawa. ON. 52 pp

Boisvert, J.B., Dyer, J.A., Lagace, R. and Dube, P. A. 1992. Estimating water-table fluctuations with a daily weather-based water budget approach. Can. Agric. Eng. **34:** 115 - 124.

Corre, M.D., Pennock, D.J., van Kessel, C. and Elliott, D.K. 1999. Estimation of annual nitrous oxide emissions from a transitional grassland-forest region in Saskatchewan, Canada. Biogeochemistry **44:** 29-49

Dodds, G.T., Madramootoo, C.A. and Serem, V.K. 1998. Predicting nitrate-N leaching under different tillage systems using LEACHM and NTRM. ASAE. **41(4):** 1025–1034.

Dyer, J.A. and Mack, A.R.1984. The Versatile Soil Moisture Budget Version Three. Tech. Bull. 1984-1E. Research Branch, Agriculture Canada. Ottawa, ON. 24pp.

Flerchinger, G.N. 2000. The Simultaneous Heat and Water (SHAW) Model: Technical Documentation. Technical Report NWRC 2000-09. [Available] Online: http://afrsweb.usda.gov/SP2UserFiles/Place/53620000/ShawDocumentation.pdf [2011, May 20]

Flerchinger, G.N. and Saxton, K.E. 1989. Simultaneous heat and water model of a freezing snow-residue-soil system I. Theory and development. Trans. of ASAE. **32(2):** 565-571.

Hayashi, M., Jackson, J.F. and Xu, L. 2010. Application of the Versatile Soil Moisture Budget to Estimate Evaporation from Prairie Grassland. Canadian Water Resources Journal. **35(2):** 187-208

Hayhoe, H.N., Pelletier, R.G. and Van Vliet, L.P.J. 1993. Estimation of snowmelt runoff in the Peace River region using a soil moisture budget. Can. J. Soil Sci. **73:** 489-501.

Kashyap, P.S. and Panda, R.K. 2001. Evaluation of evapotranspiration estimation methods and development of crop-coefficients for potato crop in a sub-humid region. Agricultural Water Management. **50:** 9-25.

Lopez-Urrea, R., Martin de Santa Olalla, F., Fabeiro, C. and Moratalla, A. 2006. Testing evapotranspiration equations using lysimeter observations in a semiarid climate. Agricultural Water Management. **85:** 15–26.

McGinn, S.M. and Shepherd, A. 2003. Impact of climate change scenarios on the agroclimate of the Canadian prairies. Can. J. Soil Sci. **83:** 623–630.

Monteith J. L. 2000. Agricultural Meteorology: evolution and application. Agricultural and Forest Meteorology. **103**: 5-9

Pereira, A.R., Sentelhas, P.C., Folegatti, M.V., Villa Nova, N.A., Maggiotto, S.R. and Pereira, F.A.C. 2002. Substantiation of the daily FAO-56 reference evapotranspiration with data from automatic and conventional weather stations. Revista Brasileira de Agrometeorologia. **10:** 251–257.

Qian, B., DeJong, R. and Gameda, S. 2009. Multivariate analysis of water-related agronomic factors limiting spring wheat yields on the Canadian prairies. Europ.J.Agronomy **30:** 140-150.

Ritchie, J.T. and Otter, S. 1985. Description and performance of CERES-wheat: A user-oriented wheat yield model. U.S. Department of Agriculture, Agricultural Research Services, ARS-38,pp. 159-170.

Robertson, G.W. 1968. A biometeorological time scale for a cereal crop involving day and night temperatures and photoperiod. Int. J. Biometeorol. **12**: 191–223.

Saiyed, I.M., Bullock, P.R., Sapirstein, H.D., Finlay, G.J. and Jarvis, C. K. 2009. Thermal time models for estimating wheat phenological development and weather-based relationships to wheat quality. Can. J. Plant Sci. **89:**(3) 429-439.

Sands, P.J., Hackett, C. and Nix, H.A. 1979. A model of the development and bulking of potatoes (Solanum tuberosum L.). I. Derivation from well-managed field crops. Field Crops Res. **2:**309- 331.

Shaykewich, C.F. 1995. An appraisal of cereal crop phenology modelling. Can. J. Plant Sci. **75:**329-341.

Shaykewich, C.F. 2001. Estimation of Ground Cover and Phenological Development of Canola from Weather Data. Manitoba Agriculture, Food and Rural Initiatives. [Available] Online: http://www.gov.mb.ca/agriculture/research/ardi/projects/98-201.html [2011, June 2]

Sheppard, S.C., De Jong, R.; Sheppard, M.I., Bittman, S. and Beaulieu, M.S. 2007. Estimation of ammonia emission episodes for a national inventory using a farmer survey and probable number of field working days. Can. J. Soil Sci. **87:** 301-313.

Suleiman, A.A. and Hoogenboom, G. 2007. Comparison of Priestley–Taylor and FAO-56 Penman–Monteith for daily reference evapotranspiration estimation in Georgia, USA. Journal of Irrigation and Drainage Engineering. **133:** 175–182.

USDA-NRCS 2004. National Engineering Handbook- Part 630. Hydrologic Soil-Cover Complexes. [Online] Available: http://irrigationtoolbox.com/NEH/Part630_Hydrology/H_210_630_09.pdf [2011, June 14]

Xing, Z., Chow, L., Meng, F.R., Rees, H.W., Stevens, L. and Monteith, J. 2008. Validating evapotranspiration equations using Bowen Ratio in New Brunswick. Maritime Canada. Sensors. **8:** 412–428.

5.0 Overall Synthesis

5.1 Significance

Seasonal fluctuations of soil moisture influenced by the extreme variability of weather parameters have huge effects on agricultural production and other aspects of human endeavour. The occurrence of drought and flood are manifested by soil moisture variation. Even the location and timing of severe weather such as hailstorms and tornadoes have been linked to variability in soil moisture (Hanesiak et al. 2004). Knowledge of soil moisture content is critical for many farm operations and the excess or deficit of plant available water is one of the most important factors that determine crop growth and development which ultimately limits crop yield. By actively monitoring soil moisture, farmers would be able to make more informed decisions about which crop to grow and which seeding date and rate would optimize crop water use (Gervais, 2008).

A continuous soil moisture monitoring network is important to fill the knowledge gap in soil moisture dynamics. In this study, a total of 13 soil moisture monitoring sites were established using FDR sensors in central and eastern Manitoba in 2009 and 2010 for the purpose of testing the VSMB soil moisture model. The sensors output hourly and daily soil moisture values. However, to ensure that the outputs from these sensors are comparable to observed soil water content, they were calibrated in the laboratory and in the field using categories based on percent clay content of the soil. Default factory parameters were found to be comparable to the laboratory derived parameters but showed significant

differences when compared to field calibration, especially in heavy textured soils. Generally, the accuracy of the default factory calibration decreased as the soil clay content increased. This study affirmed the need for site-specific calibration of the sensors especially when used in fields with heavy clay soil and when a high degree of accuracy is required.

A network of soil moisture monitoring locations provides the basis for comparing agrometeorological models to observed values. These sensors however, give point measurements; are quite expensive and often require a level of expertise for proper installation. To fill this gap, models are employed. Models are able to overcome the shortcomings of point data from direct soil moisture measurement which do not integrate these measurements over space and time as is often required in many agronomic applications (Akinremi and McGinn 1996). The suitability and use of models depends on how accurately they predict the phenomena they simulate.

Modifications were made to the VSMB, an operational model that monitors soil moisture status, to improve its accuracy. The Hargreaves equation which was used to predict solar radiation was replaced by direct solar radiation values from pyranometers. Also, ET_o determination which is an important input to the model was modified by replacing the Priestley-Taylor equation with the Penman-Monteith (FAO 56) equation. This study showed that PT underestimated the amount of water loss to the atmosphere when compared to the PM – FAO 56. However, this difference in ET_o did not result in significant difference in the VSMB soil moisture output. The model was most effective at simulating soil moisture

content at the rapidly changing surface layers. However, it largely underestimated soil moisture at lower depths in the soil profile when compared to values from the calibrated FDR sensors.

Improving the accuracy of the VSMB holds great potentials for many agriculture and hydrology related applications. Monitoring soil water and providing real-time estimates is vital to understanding drought, floods as well as severe weather forecasting on a municipal, provincial and national basis.

5.2 Future Work

Suggested improvement to the calibration methodology would be to increase the number of gravimetrically-determined data samples alongside the soil moisture sensors. This will help to boost confidence in the calibration result because more data points would provide a more representative calibration equation. Also, a long-term comparison of year to year variation of the FDR sensors should be studied. This is based on the shrink-swell cycles in the soil, especially those with high clay content, and the seasonal freeze-thaw changes, both of which can cause cracks and air gaps next to the sensors. Such study will further help to determine the degree to which the physical disruption of the soil may be affecting probe-soil contact and causing errors in the observed soil moisture values. The best installation practice for long-term soil moisture monitoring is yet to be determined.

Although the ET_o subroutine modification in the VSMB carried out in this study is a step in the right direction, the model requires further modification in order to provide accurate soil moisture values. Inclusion of the influence of depth to water table for fields with shallow water table is expected to improve the model's soil moisture prediction at depths. The model is also limited by the assumption that soil drains from saturation to field capacity in one day. This is not the case in heavier soils that often remain at moisture content higher than field capacity for some days.

There is little documentation about research that focused on the drying curve coefficients and their adaptation to the VSMB. Hayashi et al (2010) reported the coefficients $C_m, C_n, C_h \; and \; C_r$ as dimensionless fitting parameters used to derive the empirical drying curve function. Further research that looks at improving this function by deriving coefficients that are adaptable for various soil types would be a step in the right direction. The interaction of root extraction coefficients for various crops with the drying curve coefficient also requires further study.

5.3 References

Akinremi, O.O. and McGinn, S.M. 1996. Usage of soil moisture models in agronomic research. Can. J. Soil Sci., **76:** 285–29.

Gervais, D.M. 2008. Assessment of the Second-Generation Prairie Agrometeorological model's performance for spring wheat on the Canadian Prairies. M.Sc. Thesis, University of Manitoba. [Online] Available: [2010 December 23]

Hanesiak, J.M., Raddatz, R.L. and Lobban, S. 2004. Local initiation of deep convection on the Canadian Prairie provinces. Boun. Layer Met. **110:** 455-470.

Hayashi, M., Jackson, J.F. and Xu, L. 2010. Application of the Versatile Soil Moisture Budget to Estimate Evaporation from Prairie Grassland. Canadian Water Resources Journal. **35(2):** 187-208

6. APPENDICES

A PROTOCOL FOR FIELD CAPACITY AND BULK DENSITY DETERMINATION

A.1 Introduction:

The pore space of soil is about 50% of the total soil volume while the soil matrix occupies the rest. Both the soil air and soil water occupy the pore spaces. However, under saturated conditions, all the pore spaces are filled with water, forcing the air out. But as the water drains gradually, the soil air fills the spaces.

A.2 Field Capacity:

Field capacity is the amount of soil moisture or water content held by the soil after excess water has drained out and the rate of downward movement has materially decreased, which usually takes place within 2–3 days after a rainfall or irrigation event has saturated the soil depending on the texture of the soil. The physical definition of field capacity (expressed symbolically as θ_{fc}) is the water content retained in soil at 0.03 MPa of hydraulic head or suction pressure.

The field capacity varies in different soils. In sandy soils, it is between 10-20% volumetric water content (VWC), and between 30-40% VWC for clay soils. Loamy soils vary between 15-35% VWC.

A.2.1 Materials and Method:

The aim of field capacity determination is to saturate the soil with water and allow it to drain by gravity. This process was done in two stages:

a) **Saturation**: To achieve this, it is important to estimate the amount of water that will be needed. This is done by calculating the soil porosity given as:

$$Porosity = \left(1 - \frac{bulk\ density}{particle\ density}\right)$$

Therefore, the bulk density of the soil should be determined using the auger meant for this purpose (see bulk density protocol below, if unknown however, 1.25g cm^{-3} can be used for loam soils and increased for sandy soils). The assumed particle density of 2.65g cm^{-3} can be used. The bulk density and porosity determination are used to estimate the amount of water required for the soil to attain saturation.

Example: Calculate the porosity and the volume of water that will be needed to saturate a soil of 1m depth within an area of $1m^2$ with bulk density of 1.2g cm^{-3} and volumetric water content of 0.25?

Porosity = 1 – (soil bulk density / soil particle density)

Soil Particle Density value is **2.65 g cm^{-3}** is often used.

Porosity (f) = 1- (1.2 g cm^{-3} / 2.65 g cm^{-3}) = 1 – 0.45 = ***0.55.***

NOTE: Porosity is dimensionless and can be given in terms of proportion or percentage.

Of the 0.55 pore space (soil porosity), 0.25 is currently occupied by water- i.e. soil volumetric water capacity. The present pore space left to be occupied will be 0.55-0.25 = 0.30. Thus, the additional amount of water to saturate the soil is given as,

0.30 x 10^6 cm^3 = 300, 000 cm^3 = ***300 liters.***

From the calculation above, it can be inferred that soil bulk density has an inverse relationship with the volume of water needed to bring the soil to saturation (the higher the bulk density of a soil, the lower the volume of water needed to bring it to saturation). A frame of $1m^2$ internal area of any convenient height can be used to restrict surface water flow. A portion of the square frame is buried on a flat surface of the field (to avoid surface run-off) and the pre-

determined volume of water is applied gradually. Sub-surface flow of water to adjacent dry soils cannot be totally controlled since water flows in response to potential gradient.

To ensure that the spot where the reading will be taken is adequately saturated, holes may be dug around the spot to the desired depth. This will slightly increase the amount of water needed. The volume of each hole which is equivalent to the volume of additional water needed is calculated by:

$V = \pi r^2 h$ where π is pie (3.14), r is the radius of the auger and h is the depth.

Infiltration will take more time in fine-textured soils. However, adding all the water at once will create a huge pressure that the soil under the frame may not withstand, thus causing surface run-off to adjacent soils. Though run-off may not be totally prevented in some cases, it can be minimized with gradual application of water.

Once the estimated volume of water is added, the frame should be covered with a bag to prevent rapid loss to evaporation.

b) **Measurement:** After 2-3 days, the water is expected to have drained down the soil profile by gravity. Soil samples for field capacity (as well as soil bulk density, if desired) are taken from the reserved spot. For field capacity determination, only a fraction of the soil at the desired depths is needed. However, for bulk density determination, all the soil from the desired depth is needed. The table below (Table A1) shows the calculation for field capacity, given in the 10th column, assuming that the soil was earlier saturated and allowed to drain by gravity.

Based on the procedure, field capacity can be calculated as:

$$\Theta_v = \Theta_g \times P_b$$

where

Θ_v is the Volumetric Water Content at Field Capacity

Θ_g is the Gravimetric Water Content (D, 10th column in the table below)

$\mathbf{P_b}$ is the Bulk Density.

A.3 Bulk Density:

This is dependent on the proposed soil depth range. In this test-case, the use of Flat-Bottom Auger (excavation method) is explained with the aid of the table below:

Table A1: Bulk density determination from a Canola field.

Depth (cm)	From (cm)	To (cm)	Depth Diff (h)	Auger radius (cm)	Total Soil Vol V_T= ($\prod r^2 h$)	Wet Soil(*g*), A	Dry Soil(*g*), B	Moisture (*g*), C= A-B	%Moisture D= C/B *100	% Dry Mass, k=100-D	Total Wet Mass (g), MT	Total Dry Mass, Ms= (k/100)*MT	Bulk Density, $\varrho_b = M_s/V_T$
0-10	0.0	9.4	9.40	5.75	975.9	258.4	202.5	55.9	27.6	72.4	1490.3	1079.0	1.11
15-25	16.1	22.7	6.63	5.75	688.7	327.8	249.6	78.2	31.3	68.7	1177.9	809.1	1.17
30-40	31.0	38.4	7.43	5.75	771.7	273.5	205.6	67.9	33.0	67.0	1266.6	848.3	1.10
45-55	44.6	54.4	9.80	5.75	1017.4	400.0	304.5	95.5	31.4	68.6	1708.9	1172.7	1.15
95-105	96.2	106.0	9.80	5.75	1017.4	398.0	309.2	88.8	28.7	71.3	1902.1	1355.9	1.33

Result from a Canola field in Oakville on June 3rd, 2009.

STEPS:

1. Have a depth range based on the nature of the research.
2. Using the flat-bottom auger, take out as much soil in the preferred spot as possible based on the depth range. From the table above, the depth difference (6.63cm) for the 15-25cm range is not as good a representation as that of the 0-10cm depth with difference 9.40cm. (NOTE: The depth is measured 3-4 times at different sides of the hole and the average value is recorded. Thus, values under the second and third columns are averages of measured depths).
3. The auger radius (which is equivalent to the radius of the hole) is used to calculate the total volume of soil in each depth. The depth difference in each depth range is used as the height ***h*** in calculating the Soil Total Volume.

4. **ALL** the soil from each depth is weighed and recorded to give the Total Wet Mass found in the 12th column.
5. A representative sample from the weighed Total Wet Mass for each depth is taken, weighed and oven dried at 105^0C to determine its % moisture which is the Gravimetric water content.
6. The % Dry Mass is 100 - % Moisture. Thus, the proportion of the Soil Total Volume in each depth that will be Dry Mass as shown in the 13th column is given as:

   Total Dry Mass = (%Dry Mass X Total Wet Mass) / 100.
7. The bulk density is calculated by dividing the Total Dry Mass by the Total Volume.

The gidding hydraulic soil probe machine can be used in place of the flat bottom auger for soil excavation at depths. It is easier and faster, however, heavy compaction of clay soils and 'fall out' of sandy soils from the sampling tube are key challenges in using this machine.

The main limitation associated with using the flat bottom auger is the inability of the auger to collect **all** the soil grains at lower depths.

6.2 Appendix B – Hydra Probe Calibrations

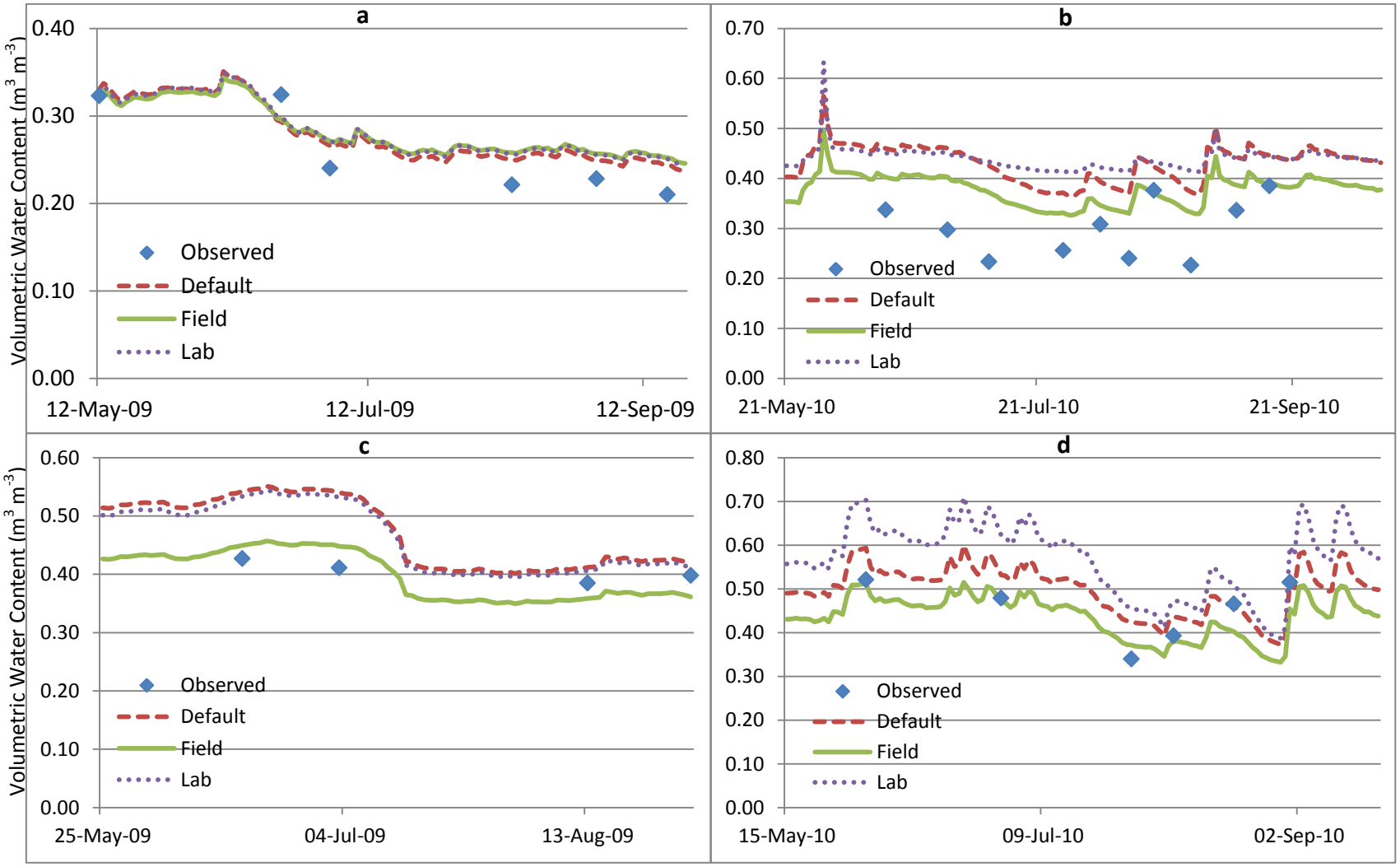

Figure B.1 Time-series comparing the moisture content derived from the default factory, field and laboratory calibrations at (a) Gladstone 2009, (b) Carman 2010, (c) Portage 2009 and (d) Kelburn 2010 fields at 20cm depth.

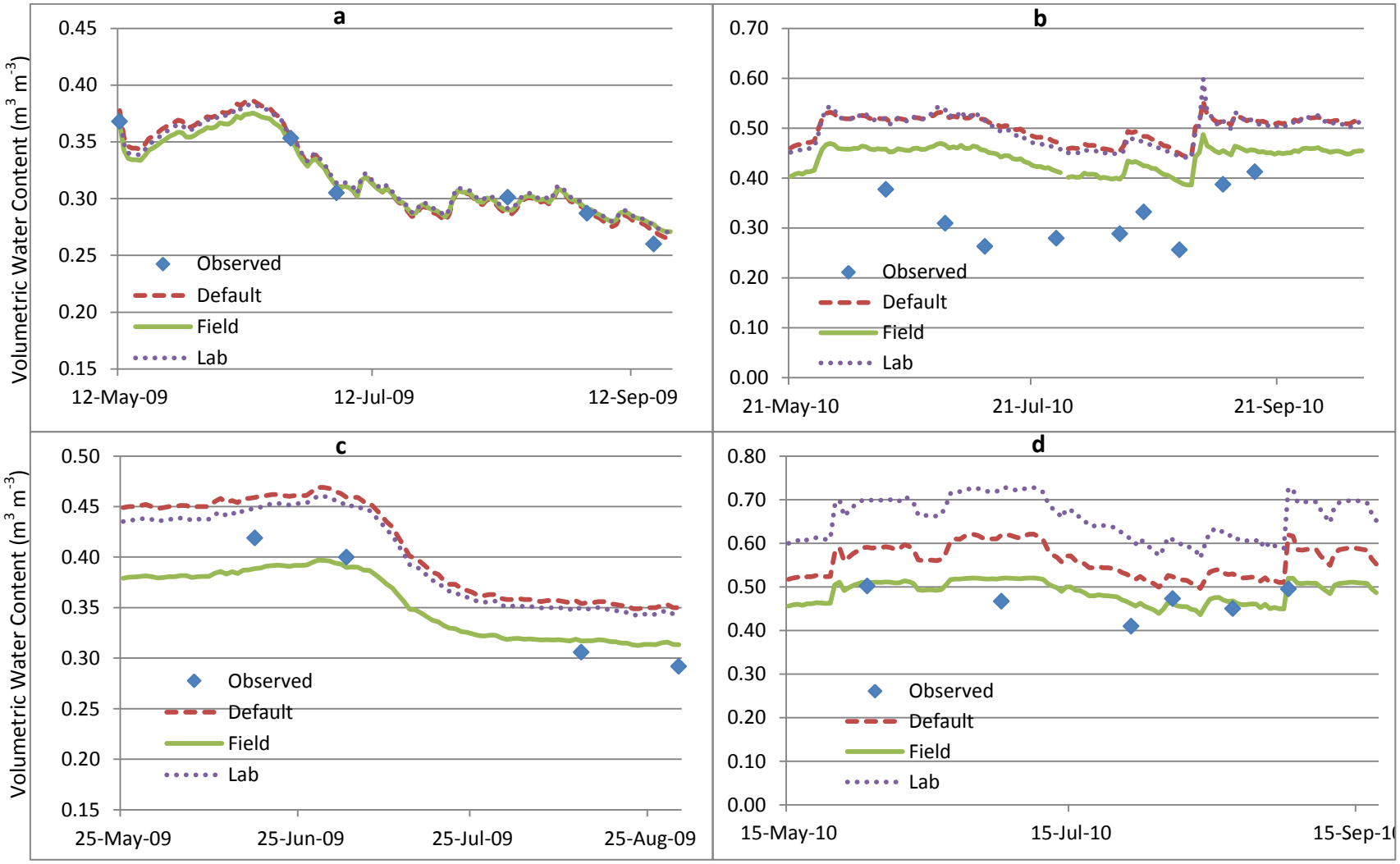

Figure B.2 Time-series comparing the moisture content derived from the default factory, field and laboratory calibrations at (a) Gladstone 2009, (b) Carman 2010, (c) Portage 2009 and (d) Kelburn 2010 fields at 50cm depth.

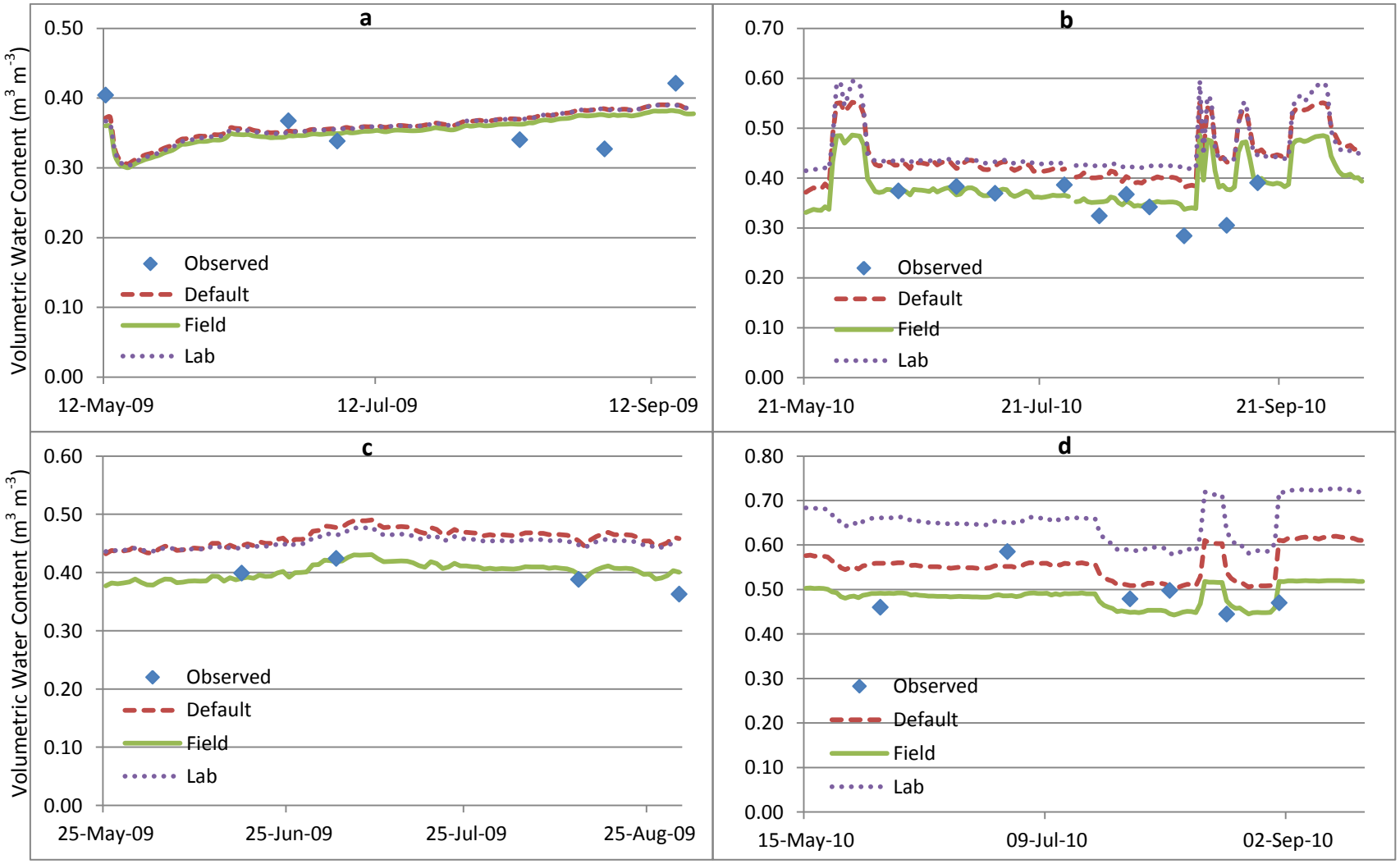

Figure B.3 Time-series comparing the moisture content derived from the default factory, field and laboratory calibrations at (a) Gladstone 2009, (b) Carman 2010, (c) Portage 2009 and (d) Kelburn 2010 fields at 100cm depth.